www.maajournal.com

Mediterranean Archaeology and Archaeometry
Vol. 23, No 1, (2023), pp. 135-164
Open Access. Online & Print.

DOI: 10.5281/zenodo.7604954

NOVEL ARCHAEOMETRICAL AND HISTORICAL TRANSDISCIPLINARY INVESTIGATION OF EARLY 19th CENTURY HELLENIC MANUSCRIPT REGARDING INITIATION TO SECRET "PHILIKE HETAIREIA"

Liritzis, I.[1,2,3,4], Iliopoulos, I.[5], Andronache I.[6], Kokkaliari, M.[5], Xanthopoulou, V.[5,7]

[1]Laboratory of Yellow River Cultural Heritage, Key Research Institute of Yellow River Civilization and Sustainable Development & Collaborative Innovation Center on Yellow River Civilization, Henan University, Kaifeng 475001, Minglun Road 85, China
[2]European Academy European Academy of Sciences & Arts, Class IV (Natural Sciences), St. Peter-Bezirk 10, A-5020 Salzburg, Austria
[3]Edinburgh University, School of History, Classics and Archaeology, College of Arts, Humanities & Social Sciences, Dept of Archaeology, Edinburgh EH8 9AG, Scotland
[4]Rhodes University, Dept of Physics & Electronics, Makhanda (Grahamstown) 6140, Eastern Cape, South Africa
[5]Department of Geology, Patras University, 265 04 Rio Patra, Greece
[6]Research Center for Integrated Analysis and Territorial Management – CAIMT4-12, Faculty of Geography, University of Bucharest, Regina Elisabeta Avenue, Bucharest, 3rd district,030018, Romania
[7]Laboratory of Electron Microscopy and Microanalysis, School of Natural Sciences, University of Patras, Rio, Patras, Greece

Received: 23/09/2022
Accepted: 25/01/2023
Corresponding author: I.Liritzis (liritzis@henu.edu.cn; ioannis.liritzis@euro-acad.eu)

ABSTRACT

A new handwritten twenty pages' manuscript of initiation to the Greek secret "friendly society" organization which was formed beginning of 19th century and essentially established the Greek independence against the Turks has been investigated. Historical accounts, spectroscopy analysis using Raman, X Ray Fluorescence and Near Infrared, for paper and ink characterization, as well as radiocarbon dating, and fractal of Minkowski Dimension algorithm of 5-lines and full-page handwritten text to identify number of scribers, and a novel pre-processing RGB color analysis of ink and paper identification have been applied. The investigation and results verify the dating of this manuscript to 1819, identify five types of iron gall inks, characterize the pulpwood and identify five different paper lots and four scribes from the ink content and handwritten styles of the compact five lines text and whole text pages. The results are mutually corroborated.

KEYWORDS: Iron gall ink, fractal, Minkowski, RGB, XRF, Raman, NIR, spectrum, radiocarbon, historical, spectroscopy, pulp

1. INTRODUCTION

In the context of the ardent desire to shake off the Turkish yoke and overthrow the Ottoman rule of Greece and establish an independent Greek state, and with the clear influence of the secret companies of Europe, in 1814 three Greeks meet in Odessa and decide to set up a strictly conspiratorial organization – the "Philike Hetaereia" (friendly society) - which would prepare the uprising of all Greeks. According to earlier historians, these were Emmanuel Xanthos, Nikolaos Skoufas and Athanasios Tsakalov.

All three have already become sharers of revolutionary ideas and the masons' fellowcraft. Skoufas had close contacts with Konstantinos Rados, who was initiated in Carbonarism[1]. Xanthos had been initiated into a masonic lodge of Lefkada ("Society of Free Masons" of Aghia Mavra), while Tsakalov had been a founding member of a Philanthropic Society and knew the organization of the "Hellinogloso" (Greek Language) Hotel in Paris (1809) (Katopodis 2021; Mazarakis-Aenian, 2008).

Young Phanariot Greeks from Constantinople and the Russian Empire, local political and military elites from the Greek mainland and islands, and a few Orthodox Christian leaders from other nations under Hellenic influence were among the society's members. Prince Alexander Ypsilantis, a famous Phanariote[2], was one of its leaders. In the spring of 1821, the Society began the Greek War of Independence (Phillips 1897; Koliopoulos 1987).

The members of Filiki Etaeria had to be initiated under a closely to freemasonry process. The whole initiation included a written text, which contained a verification letter (ephodiastikon), indicating that someone belonged to the Friendly Society and the Catechism text. Such documents of its members that have been saved belong to the valuable testimonies both for the character of the organization and for the characteristics of its members. As these are essentially secret identities of the Friends, they indicate the place from which the member of the Society comes, the social group and the profession, the educational level and his financial situation, but also the time of the initiation. They thus illuminate the activity of the Company as well as its geographical and social spread. The verification letters are written in cryptographic way on paper. The initiator, who usually had the rank of "Priest", gave it to the incoming member after the initiation. The Priests had an average rank in the hierarchy of the Society and mainly undertook the identification and inclusion of new members up to the rank of Priest. Only the "Invisible Authority" could initiate senior members. Upon entering the Company, the initiates offered a sum of money and a letter of dedication, where they noted in addition to their basic data and the coded initials with which they would be identified and would correspond with each other from now on (Panagiotopoulos 1964).

The present work concerns the investigation of such a handwritten document which are the property of the Grand Lodge of Greece in Athens and consists of a complete text of such initiation. The aim was to authenticate its originality, explore the content of the ink and the paper used and examine the number of authors from the handwritten style. The goals were approached by historical literature search, a combined analytical effort using Raman, X-Ray (XRF) and Near Infrared (NIR) Spectroscopy techniques, with radiocarbon dating and using Minkowski Dimension algorithm of fractal dimension and RGB color analysis for text images and words, all on a complementary manner.

2. MATERIAL & METHODS

2.1 Material

The investigation is made on a 20-page A4 manuscript with front cover and back cover written in black ink. It refers to the initiation of a new person in the "Friendly Society". This initiation was made with the oath of the Friends and included the symbolic alphabet and a verification letter to the Fellow in the rank of "priest" of the Friendly Society, signed by the catechist, and the entire Catechism text. Although under historical investigation, the present manuscript is probably unique as a whole, while the name of the newcomer *Anagnostis Parthenopoulos* is mentioned, which is also confirmed in Sekeris's archive (Mexas 1937; General State Archives of Greece[3]).(Figures 1-4). The confirmation letter mentions the date of 3 April 1819 in island of Hydra, the initiation was taken place.

The confirmation letter mentions the date of April 3, 1819 on the island of Hydra, where the initiation took place, the catechist is listed in the Sekeris archive as Nikiforos Pamboukis and the Friend who would receive it was Anagnostis Zoopoulos in Constantinople.

The "Priest" present was Anagnostis Parthenopoulos and the manuscript had on the cover the sacred

[1] informal network of secret revolutionary societies active in Italy from about 1800 to 1831 most likely emerged as an offshoot of Freemasonry (Rath 1964)

[2] Members of prominent Greek families in Phanar the chief Greek quarter of Constantinople where the Ecumenical Patriarchate is located. Phanariots were aware of their Greek ancestry and culture.

[3] http://www.gak.gr/index.php/en/

toggle with the sixteen columns, a laurel wreath and two cross spears with hanging banners. The acronyms "HEA" (i.e. or Freedom) and "ΗΘΣ" (i.e. or Death) were written on the banners. This friendly initiation has been confirmed by historical archives referred to dozens of initiated Greeks (Mexas 1937).

2.2 Sampling

All spectroscopy techniques were applied in a non-evasive manner measuring the respective radiation from a focused spot on the page, either ink or paper, for fractal analysis the image of each page used used, and for radiocarbon dating (C-14) a small square piece was removed from the back cover of the manuscript (Fig 5).

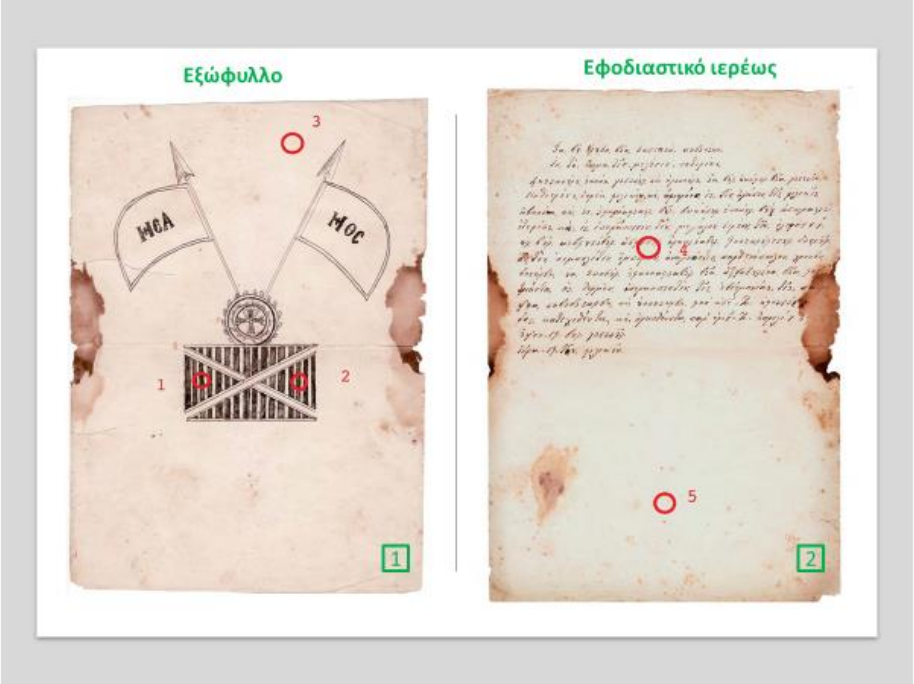

Figure 1. The front cover and verification letter (page 1)

2a

2b

2c

Figure 2. a) The signs of greeting hands, the Great Oath, cryptographic alphabet and other text (pages 2-7), b) more pages of text (8-13), c) pages 14-18 and back cover.

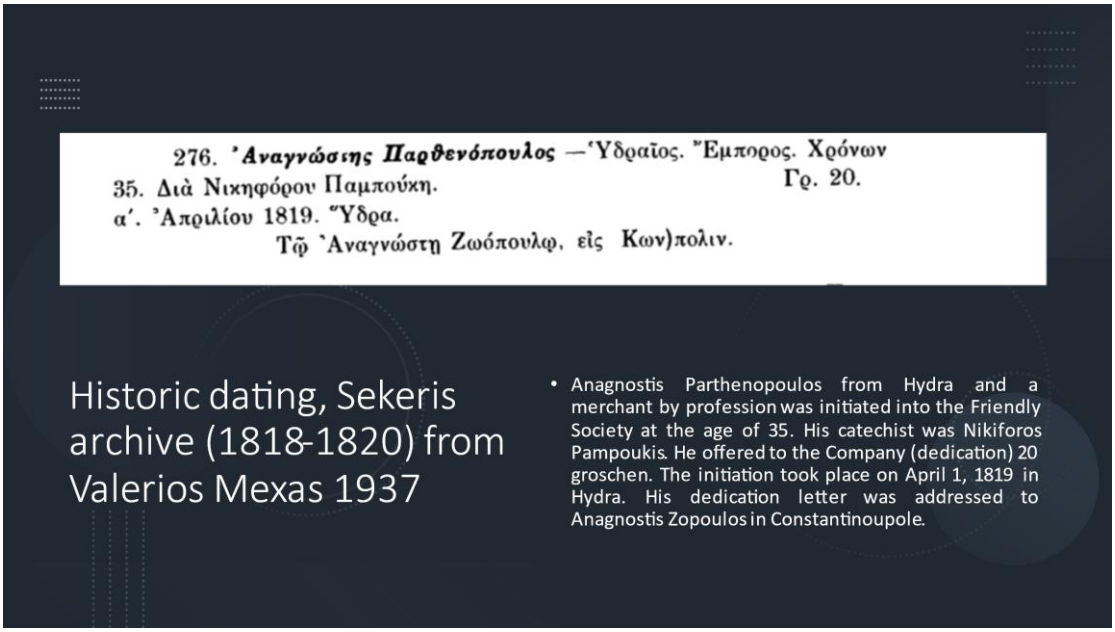

Figure 3. Historical evidence of the studied folios as written for an initiation of Mr Anagnostis Parthenopoulos on April 1819. Upper: Extract from the Sekeris archive (1818-1820) (Mexas 1937). The recorded extract of Sekeris archive, Right: Transliteration.

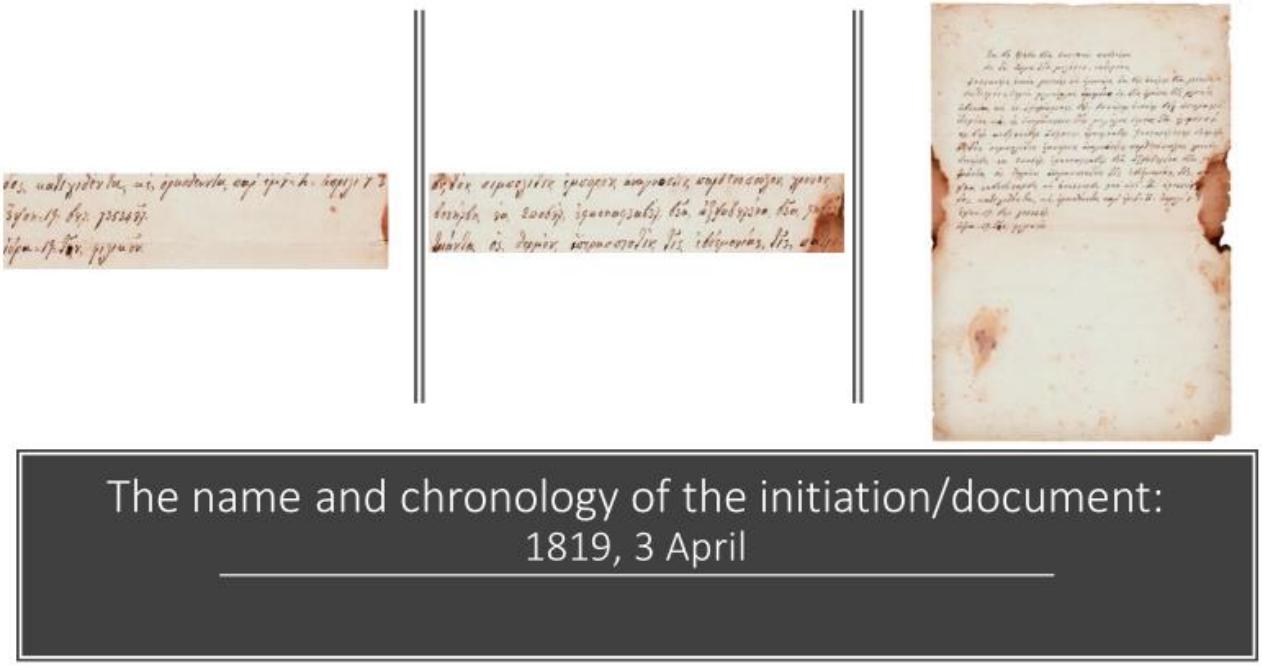

Figure 4. Sentences of the text showing the date (3 April 1819) in the confirmation letter of page 1. Left: the date, Middle: the name, Right: the page.

3. METHODS & INSTRUMENTATION

3.1 XRF

Selected spots on the paper surface is analyzed by means of XRF/EDS using a NEX CG, Rigaku system (LEMM) with an X-ray tube with Pd anode which worked under a tube power of 50W (50 kV to 2mA). It is equipped with 5 secondary targets and a Silicon Drift Detector (SDD). Standardless analysis performed using RPF-SQX (Rigaku Profile Fitting – Spectra Quant X) software with a fundamental parameters method for accurate quantification combined with full profile fitting method (Fig.5). No compensation for variations in paper thickness/density or more gross imperfections at the exact location of an XRF

analysis was accounted; present measurements serve a semi-quantitative evaluation.

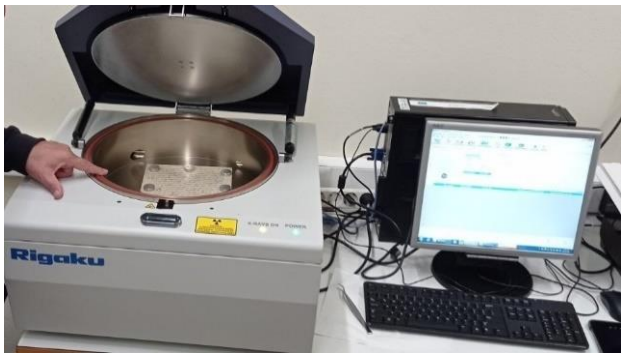

Figure 5. XRF device and paper setting for reading

The readings were taken on certain spots in each page (Fig.6)

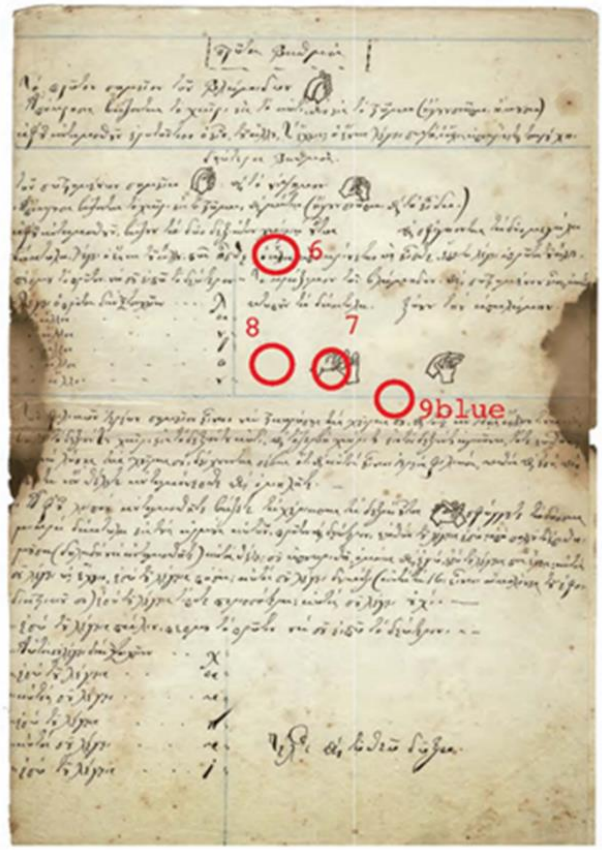

Figure 6. XRF spots where measurements were taken. Here page 3 with sketches of secret handshake sign.

3.2 Raman

The examination was conducted using a Jobin-Yvon Horiba LabRam-HR Mirco Raman spectrometer that is coupled with an Ar+ excitation source wavelength 785 nm and is equipped with an Olympus microscope (the 50× objective was used). The spectra were recorded within a 10 s acquisition time in the case of 2 successive spectral windows and on a 2micron spots (conducted at the Laboratory of Electron Microscopy and Microanalysis of the University of Patras) (Fig.7A).

3.3 NIR

The reflectance spectroscopy (SM-3500 Spectral Evolution portable spectrometer) was applied on carefully selected, smooth, unaltered surface of the hand specimens, bringing the reflectance probe spectrometer, with a field of view (FOV) 2 x 1.5 cm, in contact with the surface of the samples. The data acquired ranges from 0.35 to 2.5 μm with a spectral resolution according to the software, between 3.5 and 8 nm. The spectra were finally produced by the instrument at 1 nm intervals, using the DARWin SP Data Acquisition software, which is accompanied by the United States Geological Survey (USGS) mineral standards database. Sample spectra were first calibrated relative to a Spectral Evolution standard panel (5 x 5 cm in size) (Fig.7B).

(A)

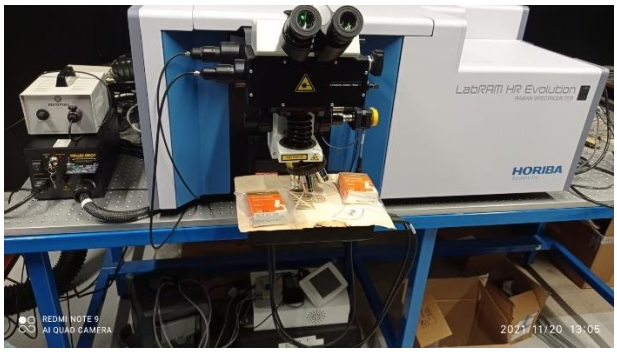

(B)

Figure 7. Raman (A) and NIR (B) settings

3.4 Radiocarbon

The measurements were made at the Keck carbon cycle AMS facility, the Earth system Science dept, UC Irvine. (c/o Dr John Southon). The samples received a standard acid-base-acid (ABA) treatment which would remove (among other things) materials like animal glue that might have been used as sizing and (more to the point) any calcium carbonate that might have been used as a filler, that could potentially bias the 14C date old. In view of the potential importance of the sample a second aliquot was run that received a bleaching treatment as well as the ABA.

4. RESULTS AND DISCUSSION

4.1 XRF results

During the chemical analysis of the historical item with the XRF system, a total of 28 measurements were performed, of which 20 in areas with ink and 8 in areas of paper, free of ink. The nine elements (S, Cl, K, Ca, Ti, Mn, Fe, Cu, Zn) were measured. Characteristic XRF spectra for ink and paper is given in Fig. 8 and the XRF data in Table 1.

Page 4 Ink

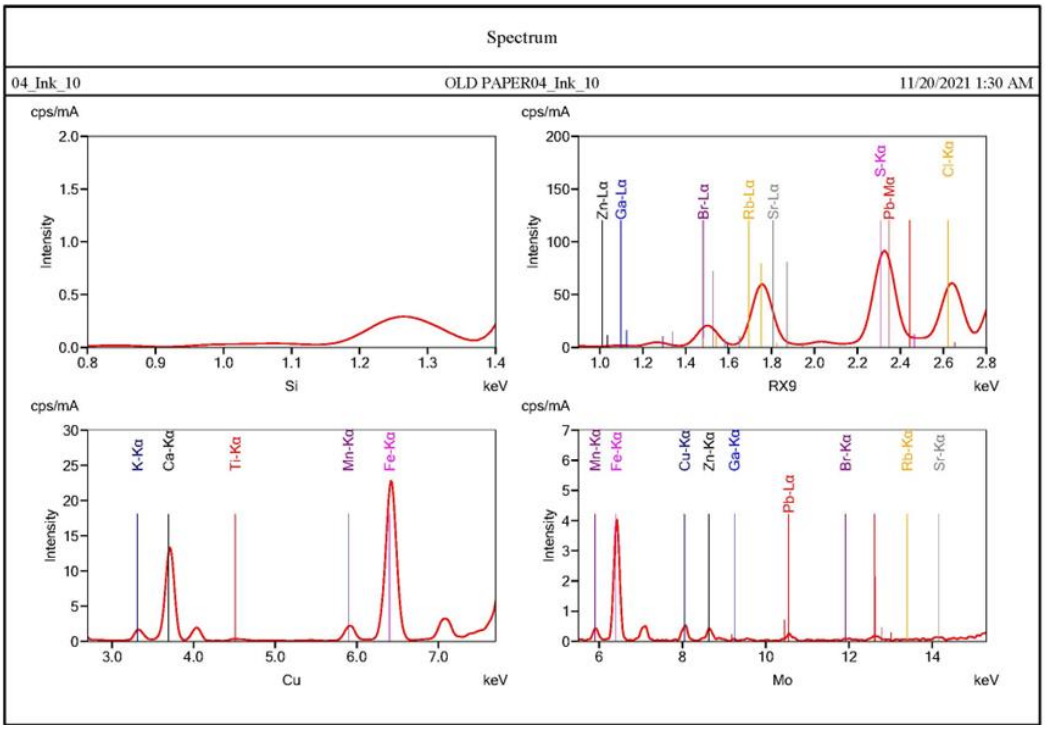

Page 4 Paper

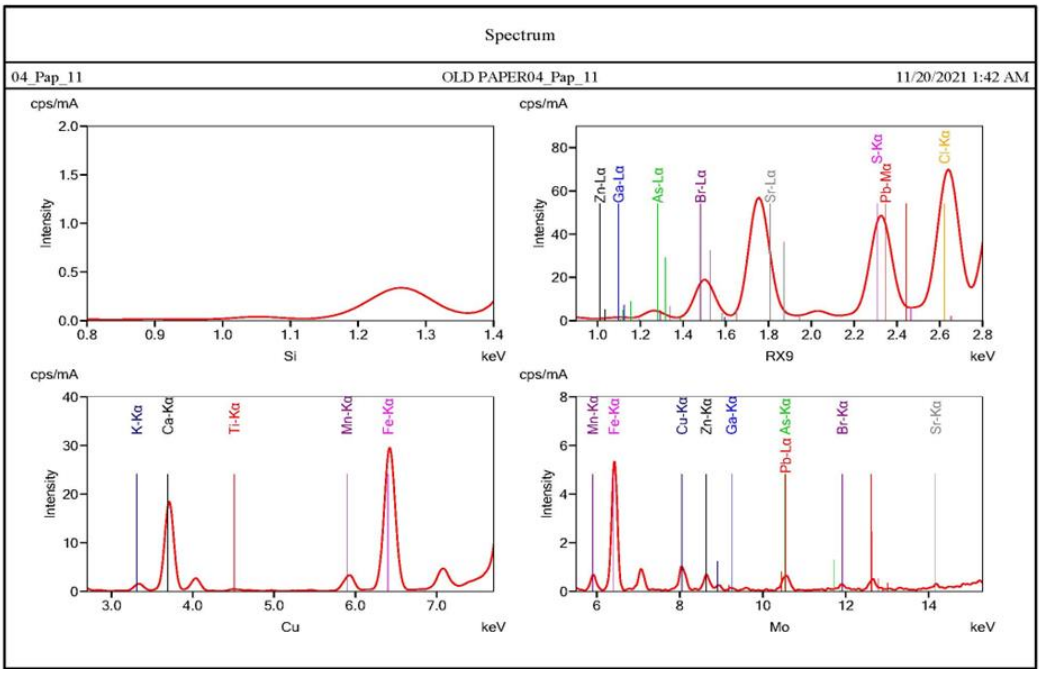

Figure 8. XRF spectra of ink and paper of page 4. Note X-rays peaks with relative intensity given in Table 1. Note X-rays peaks with relative intensity. Pages are mentioned according to the numbering of the pages in the real manuscript. Si, RX9, Cu and Mo indicate the different type of secondary targets used by the NEG CG apparatus breakthrough concept, in order to realize a polarized optical system which reduces considerably continuous X-rays, thus enabling higher sensitivity and precision than ordinary ED spectrometers.

Table 1 A) XRF elemental content in ppm per measurement for Ink or blank page. (e.g. 01-ink-01 means first page, for ink and 1st reading; 12-pap-15 means the 12th page of blank paper and the 15th reading), B) page number and A4 or A3 sheets. The additional 3 pages are unwritten these 3 are 4, 5, 6 in the numbering of all pages blank and written. The 4th paper starts with p.7. NOTES: Blue: INK Ti average of ink in the pages of the same section ie written pages 4, 5, 6, 7 pages is used because these are of same paper A3 =2A4. Green: INK Mn an arbitrary value was used close to that of the page, as follows: The elements Cu, Zn, Ti in page 1 are thrice than those of page 2. Thus Mn of page 2 is chosen arbitrarily as about thrice of page 1. The page 4 with following 5-7 consist of same A3 paper.

(A)

	S	Cl	K	Ca	Ti	Mn	Fe	Cu	Zn
01_Ink_01	164000	9290	23900	610000	838	4670	169000	5210	2840
01_Ink_02	153000	10200	26400	610000	1170	5100	175000	5460	3010
01_Pap_03	138000	12700	8440	756000	1200	7620	47500	8910	4760
02_Ink_04	83200	99600	59700	411000	3670	16320	221000	15000	10300
02_Pap_05	112000	126000	96400	434000	9570	17400	153000	19500	11900
03_Ink_06	77200	72600	54100	454000	8070	34900	233000	23100	16100
03_Ink_07	77500	64800	49200	430000	8750	27000	286000	23100	15000
03_Ink_09bl	91400	74600	56600	427000	8910	30600	246000	25600	15900
03_Pap_08	72500	71900	55500	459000	7460	36200	231000	22200	17000
04_Ink_10	132000	55300	68300	392000	6630	32800	256000	19400	13400
04_Pap_11	48600	49400	50300	439000	6440	41500	263000	38200	19000
05_Ink_12	178000	48500	93700	378000	6160	26900	217000	23800	13900
05_Ink_12R	175000	47400	87400	392000	5450	24700	211000	24600	10900
06_Ink_13	113000	57500	59000	442000	6010	34300	219000	23600	13300
07_Ink_14	86700	39800	62600	407000	6550	35200	279000	30700	17600
08_Ink_21	22700	18300	27800	211000	2990	19800	178000	392000	14200
08_Pap_20	53700	52000	43900	388000	8450	48500	294000	52600	20800
09_Ink_22	79200	46500	47300	398000	4830	40300	293000	36300	18700
10_Ink_23	104000	64200	57200	436000	6180	34300	238000	20100	17900
11_Ink_24	109000	67200	53800	451000	4550	29100	222000	23300	15800
12_Ink_16	98800	64400	60800	444000	5860	35100	223000	25000	16300
12_Pap_15	58300	59500	60000	436000	6090	33800	265000	28700	20200
13_Ink_17	69500	46700	45000	413000	6430	41800	297000	30300	19500
14_Ink_18	96100	37700	63900	388000	5110	38800	293000	30600	19000
15_Ink_19	87600	39900	58100	397000	6700	43900	286000	32400	18000
16_Ink_25	76700	43500	63100	391000	5310	39400	293000	31400	23500
19_Pap_26	62900	44500	38000	403000	7650	41500	313000	34900	21900
20_Pap_27	163000	13300	14000	736000	1370	6130	40300	9350	4040

(B)

Number of pages with red the written ones and black written and blank	**sheets**
(1) 1 front page	Single
2	Single
3, 4, 5, 6	A3=2A4
(4-7) 7-10	A3=2A4
(8-11) 11-14	A3=2A4
(12-15) 15-18	A3=2A4
(16-19) 19-22	A3=2A4
(20) 23 back page	Single

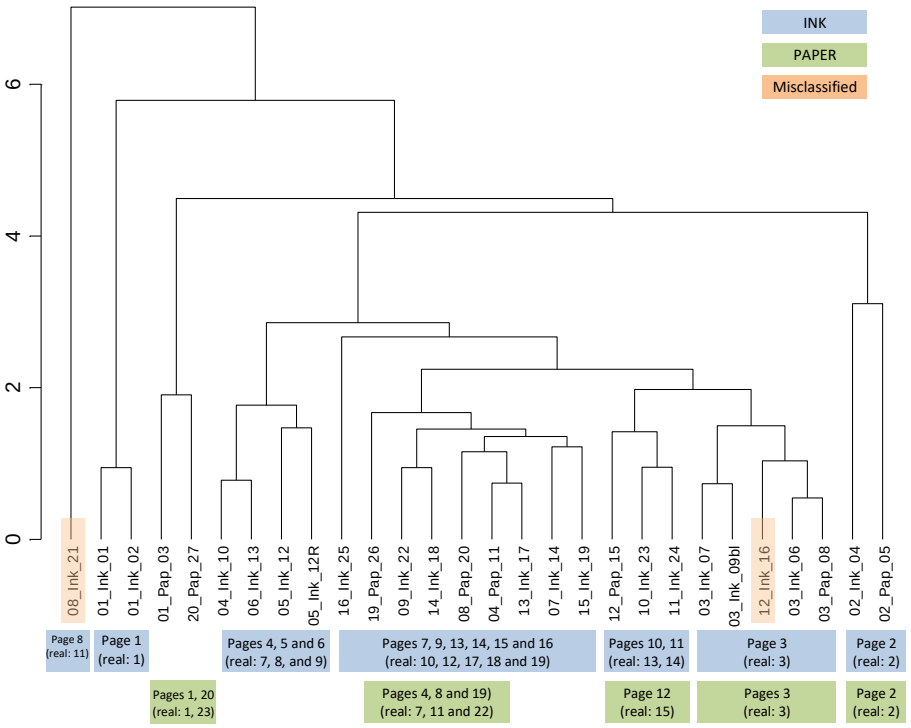

Figure 9 Dendrogram produced using Agglomerative Hierarchical Clustering (average method) performed on log ratio transformed data using Zn as a divisor (Br and Sr were excluded due to many missing values). (Real: numbering of the page includes the white pages of the big A3-like page of the original)

The statistical processing of the data was performed after their normalization using the Agglomerative Hierarchical Clustering (average method) performed on log ratio transformed data (Fig.9).

The following 3 groups are observed:

1) **GROUP 1**. A first reading of the chemical data table allows a direct distinction of the similar **front paper cover (page 1 of the item) and back cover (page 20** of the item), as well as their bearing ink, with respect to the rest of the pages. This distinction in relation to the rest of the pages is made directly on the basis of the elements Ti, Mn, Fe, Cu and Zn, while to a lesser extent also due to K and Ca. The resulting dendrogram allows also to identify the group of the front cover and back cover; the clustering for both paper and ink are displayed near left end of the diagram (Fig. 9).

2) **GROUP 2**: The rest of the analyses are displayed in the next large cluster of the diagram (04-ink-10 and right), in which **two main groupings** are identified. Of these, the **first classification** of the paper and ink of the page with the **cryptographic code (page 2 of the manuscript)** stands out at the right end of the dendrogram.

3) **GROUP 3**: The remaining data occupy the **second group**, in which the tendency of the analyses corresponding to the paper and the ink of the page bearing the **hand drawings (page 3 of the item, 03-ink-06, 03-pap-08**) can be recognized which occupies the right limit of this group.

4) **GROUP 4**: The other analyses (11-ink-24 to 04-ink-10) do not seem to indicate a clear grouping trend, but they do vaguely indicate the grouping trend between them depending on the section of the item from which they come (the section of the item means the two pages that create an A3 page).

5) **GROUP 5**: It is worth noting that **two analyses** from the total of 28 values recorded in total, either indicate a "deviated" or "extreme" value (outlier, 06_Ink_21), or are classified abnormally in relation to the other analyses of the same section of the item (analysis 12_Ink_16).

For these two "suspicious" analyses the one (06_Ink_21) is characterized by a very high Cu value (392000 ppm versus 28567 ppm which is the average of the inner pages of the item, excluding the covers and page 2). This fact probably indicates the **contamination** of the item at this point. The second suspicious XRF reading (12_Ink_16) may be related to the excessive ink spill observed at the analysis point.

The degradation is different in the pages as visually observed and validated from RGB patterns (see below), yet the chemical signature is the same (see covers of Page 1 and 20, for XRF though not verified by RGB). Hence a conclusion is that the variable decay effects per page confuses the attribution of color to

different paper. The combination of XRF with Raman and RGB color analysis elucidates these possibilities.

Another test of identifying different inks is using plots of Fe compared to Cu and Fe compared to Zn (such as Hortense de la Codre et al., 2020, figure 5).

Additionally, some ratios (such as Zn/Fe and Cu/Fe, Ti/Fe vs Cu/Fe, Zn/Fe vs Ti/Fe) may get rid of the difference of ink quantity on the paper (which can be important depending of the moment when the quill was dove in the inkpot). At any rate the XRF readings are taken on a ROI of about 1cm² thus include ink and adjacent paper and the results are taken as indicative and not precise. Yet a general trend is worth noting when compared with RGB analysis.

Indeed, the Zn/Fe vs Ti/Fe gives a group; on the left are distinct the **ink of page 1** (01_Ink_01 and 01_Ink_02), **also ink page 2** and **ink page 3 to 16** grouped. For paper on the right the **paper of page 1 and 20** seem similar (01_Pap_03 και 20_Pap_27), and up is one alone **the paper for 2nd page** 02_Pap_05. The paper 3-14 and ink 3-16 form a broadly non compact dispersed group. (Fig.10a).

In the Ti/Fe vs Cu/Fe a group along a range of Ti/Fe in the center. Regarding the inks, distinct are the two readings of **ink page 1** on the left (01_Ink_01 and 01_Ink_02), and one alone the **ink of page 8** (08_Ink_21) and the ink of pages **9 and 3.** For the paper one on the right is the **page 2 paper** (02_Pap_05), and also distinct paper of pages **1, 8, 20** (Fig.10b). The variation is due to Ti/Fe, the Cu/Fe is almost unchanged.

The Zn/Fe vs Cu/Fe a group in the center (see page numbers on the figure), and for **inks** with left again the **page 1** inks 01_Ink_01 and 01_Ink_02, **page 2**, and up alone the **8th page** ink 08_Ink_21, and inks of pages **5-6 grouped**. On the right the **paper 01_Pap_03 and 20_Pap_27,** are distinct and all others group together (Fig.10c).

For these plots the other pages for ink or paper form one group.

(A)

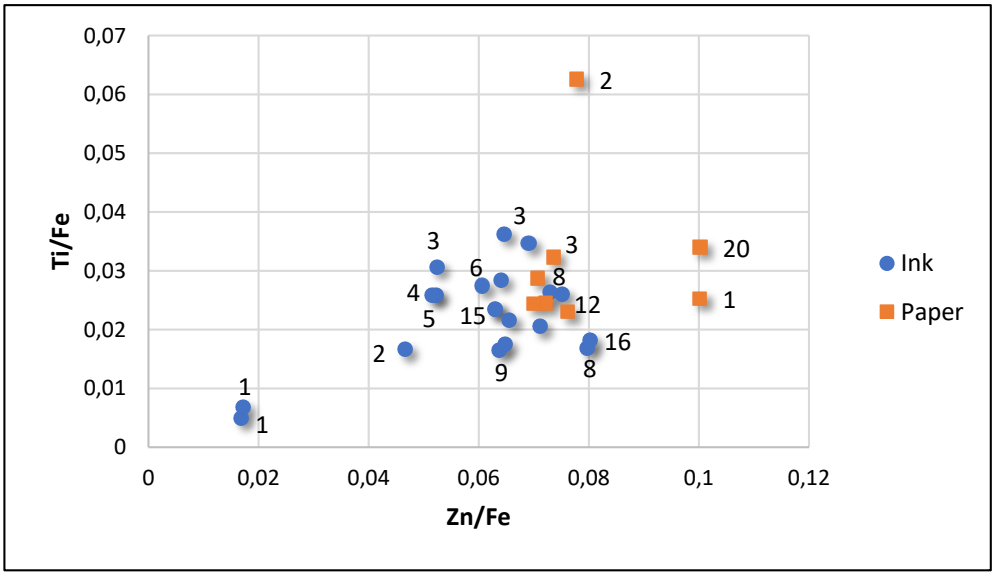

(B)

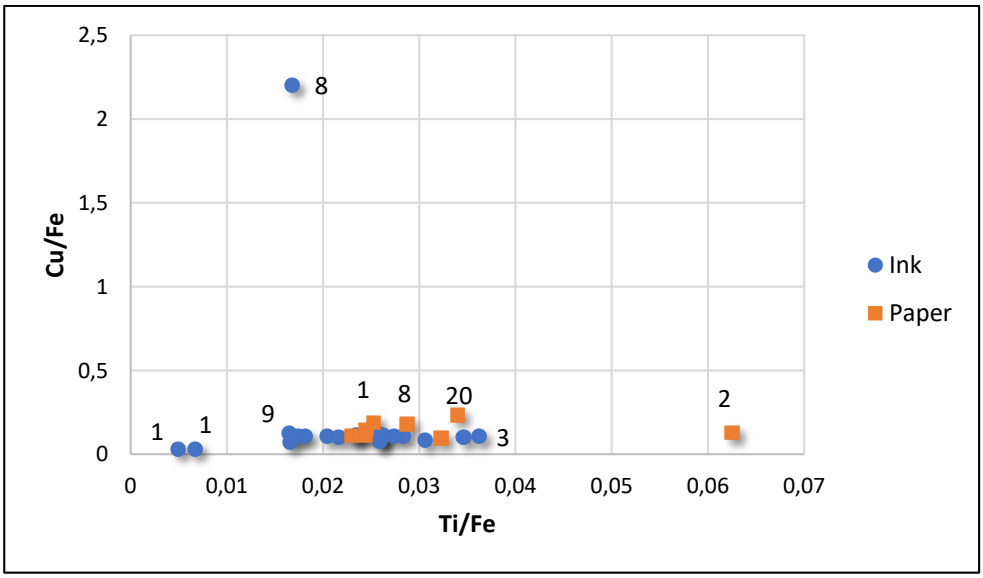

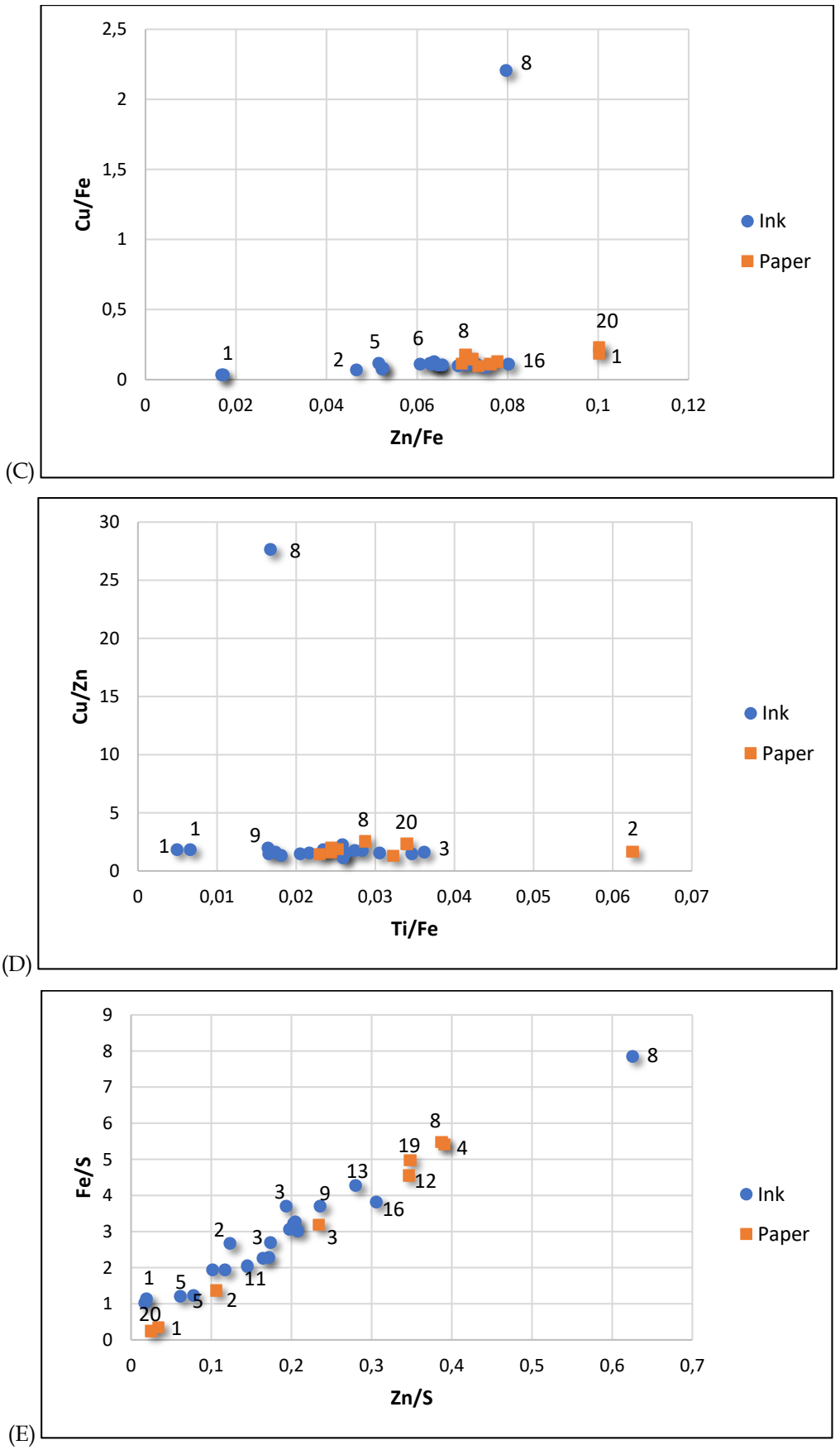

Figure 10. Elemental ratios of ink and paper. (A) Zn/Fe vs Ti/Fe, (B) Ti/Fe vs Cu/Fe, (C) Zn/Fe vs Cu/Fe, (D) Ti/Fe vs Cu/Zn and, (E) Zn/S vs Fe/S.

The Ti/Fe vs Cu/Zn: gives again a **central group** and left are again the **page 1 ink** and up the **8th page ink** and the page 9 ink and 3; other inks form a group. **Paper for page 2** alone on the right, as well as the paper of **page 8 and 20** and others form a group (Fig.10D).

Last the plot of Zn/S vs Fe/S shows a positive correlation with a distinct **ink of page 8,** 08_Ink_21, and also inks from pages 1,2, 3 (Fig.10E). For **paper** the pages 1, 2, 3, 4-19 form 4 different papers. This linear trend indicates a proportional contamination of folios with sulfur.

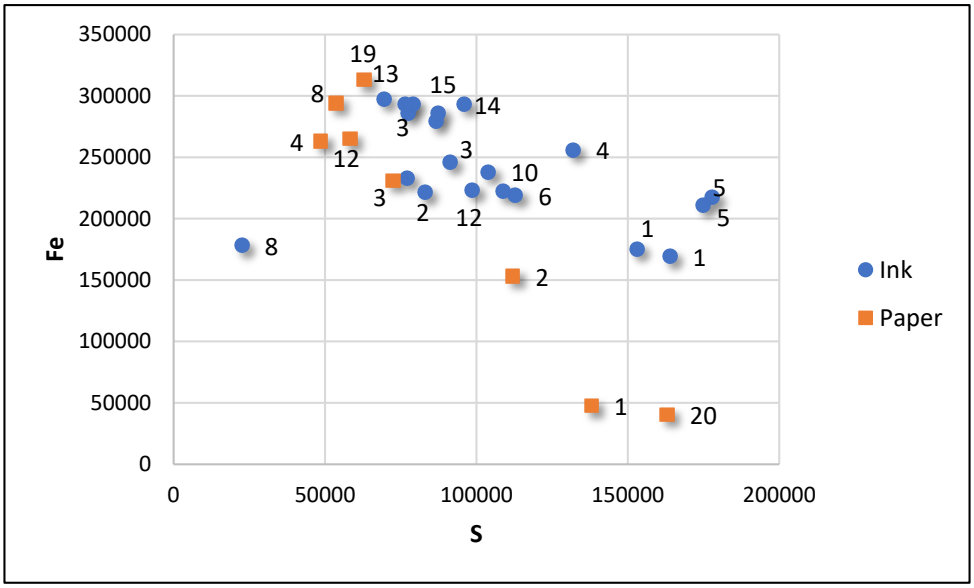

(F)

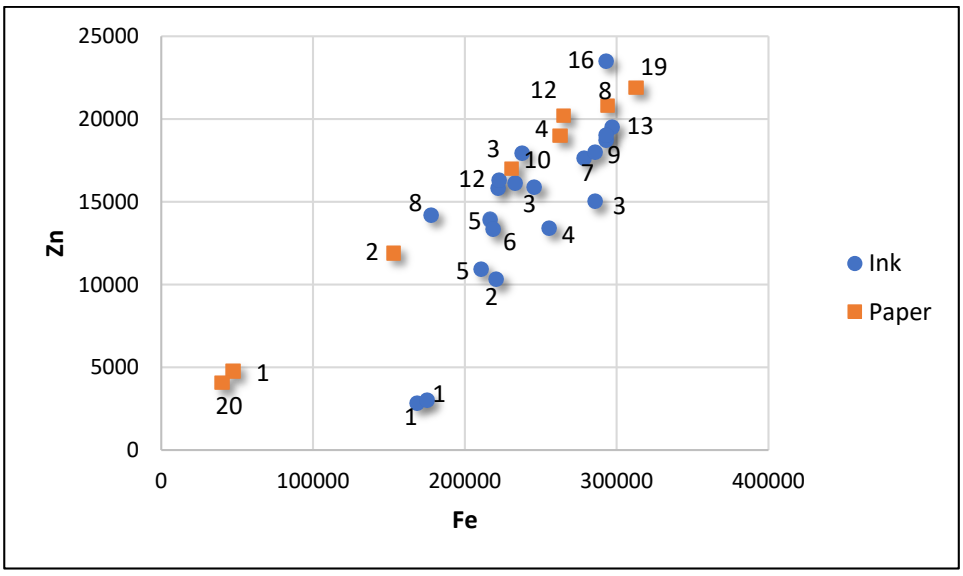

(G)

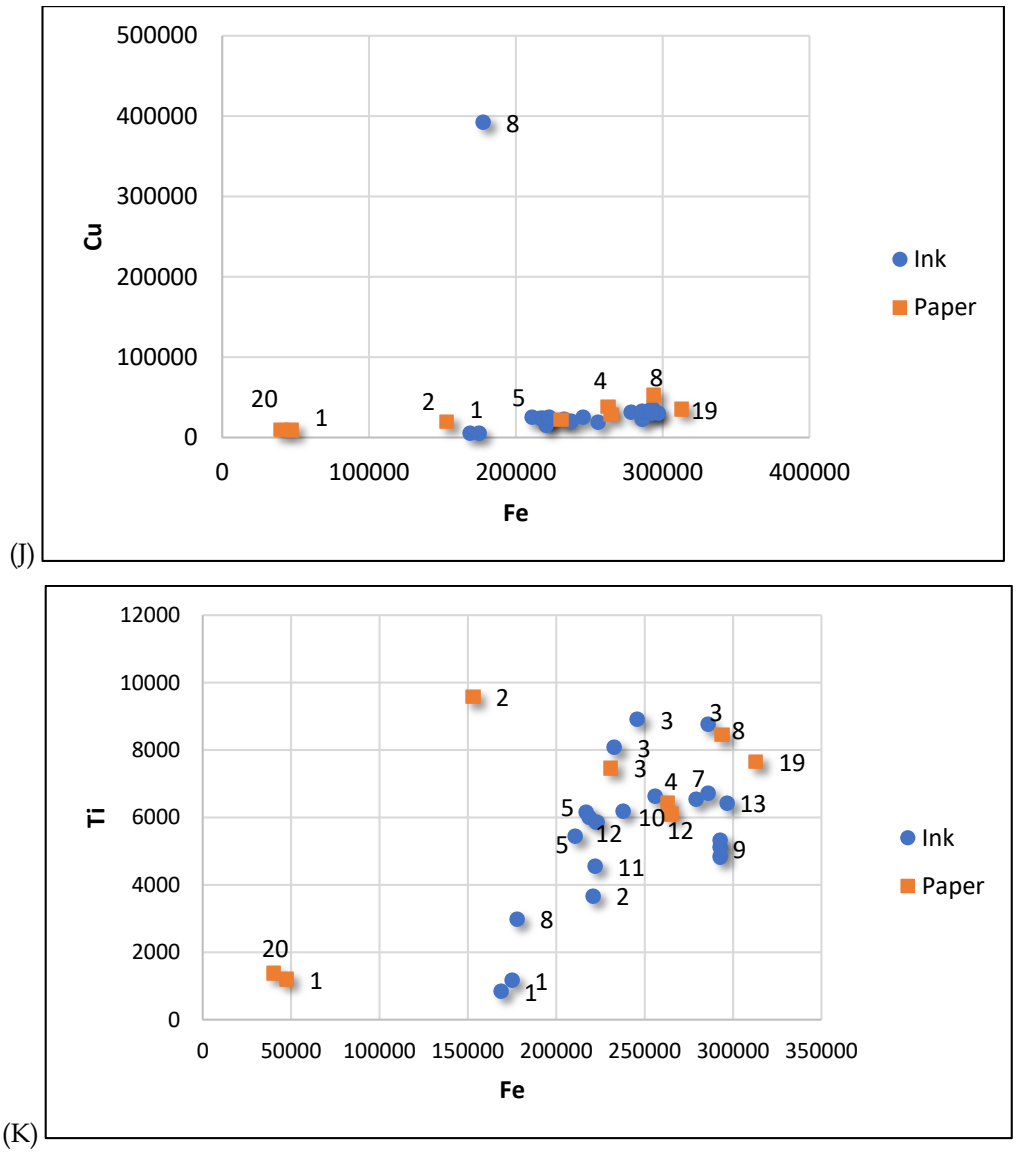

Figure 10. Elemental X-Y plots of (F) Fe-S, (G) Fe-Zn, (J) Fe-Cu, and (K) Fe-Ti.

In Figs 10 (F-K) of the plots of individual elements the following remarks are drawn:

For **Fe-S** the similar **paper** seems to be for pages 1, 2, 20 and the others form a group. For **inks** pages 1, 5, 8 and the others form a group.

For **Zn-Fe** the similar **paper** appears for 1 and 20, the 2 and 3-19 grouped. For **ink** pages 1, 2, 8 are different ink and the rest is grouped together.

For **Cu-Fe** the paper clusters for pages 1 and 20, separate for page 2, and for the inks the page 1, 8, and rest together.

For **Ti-Fe** again seem of **similar paper** the front (1) and back (20) pages, the rest grouped together, and for **ink** different ones in the **pages 1, 2, 8** and rest grouped.

Overall remark is the separate inks and papers for pages 1, 20, 2, 3, 8, 4-19. The four to five different paper types and inks are confirmed from RGB image analysis; with the difference between the methods (XRF and RGB) for page 8 and 20.

The **iron content** in various pages varied between 5-32% indicating the iron gall ink type but also the ageing and batch (lot) that the portion of the inkpot used by a scriber derives from.

Calcium carbonate powder is a bright white mineral with the chemical formula $CaCO_3$. It is used as a filler in paper pulp and as a coating pigment. The main rationale for utilizing Calcium Carbonate Powder in paper production is to improve the brightness and opacity of paper and pulp. The Ca content decreases by time and a statistically significant decrease in the mean calcium concentration over the first three centuries has been quoted elsewhere (Barrett et al., 2016, Fig.9).

Sulphuric acid H_2SO_4 is one of the raw materials used in the paper and pulp industry for the production of chlorine dioxide, a powerful oxidizing and

bleaching agent which is used for the chlorination of water. Of particular notice is the high Sulphur content in the two (perceptible thicker) covers of the manuscript (14-16%), with a low potassium ~1% content, in contract to the rest of paper pages with 4-6% and the single 2nd page with the confirmatory letter ~9%.

The XRF contents of metal residuals included **potassium and sulfur**, which are indicators of **alum**[4] concentration; **iron,** a common paper contaminant; and **calcium**, which is frequently coupled with compounds such as calcium carbonate, which can act as alkaline reserves. A survey has discovered that lighter-colored papers (closer to white) have higher quantities of gelatin and calcium and lower levels of iron. Moreover, this survey also revealed significant drops in gelatin[5] and calcium concentration across time, with the greatest variations occurring around 1500 AD, when printing became popular (Barrett et al., 2016). Higher iron levels and greater thickness are connected with worse quality papers.

Some particular elements have an anticipated positive (Ca) or negative (K, S and Fe) association to paper stability. The high values of the latter three in the manuscript concerning the paper stability is also visually verified.

The **iron, calcium, and gelatine** content appear in old papers to be more closely associated with differences in paper quality. The presence of **Chlorine** is related to the introduction of chlorine bleach around 1800 which is an important development that likely began to artificially lighten the overall colour of papers made, at least until the introduction of the first papers made from wood pulp around 1840–1850. We observe the different Cl contents in the pages – cover, 2nd and the rest, which matches with the result obtained for Fe, K, S elements.

4.2 RAMAN results

During the period ca 1780-1830 AD type of ink used were carbon and iron gall ink and regarding the paper it is the transitional phase of older production techniques (rags, and the industrially introduced pulpwood paper; the latter being used throughout the Europe after ~1840.

The Raman spectra collected from seven pages showed the use of iron-gall ink (Fig. 11). The identification of iron-gall based on bands observed at 566, 710, 815, 1098, 1230, 1333, 1481 and 1585 cm^{-1}. According to literature the position of 1341 band, which is the most characteristic for the identification of iron-gall ink, varies and can be found within the range 1350-1310 cm^{-1}. Furthermore, the band at 566 cm^{-1} varies can be found within the range 640-490 cm^{-1} (Lee et al., 2006; Carter et al., 2016).

Carbon black ink has not been detected, since it is represented by the characteristic bands at ca.1590 and 1320 cm^{-1} (Coccato et al., 2015; Carter et al., 2016).

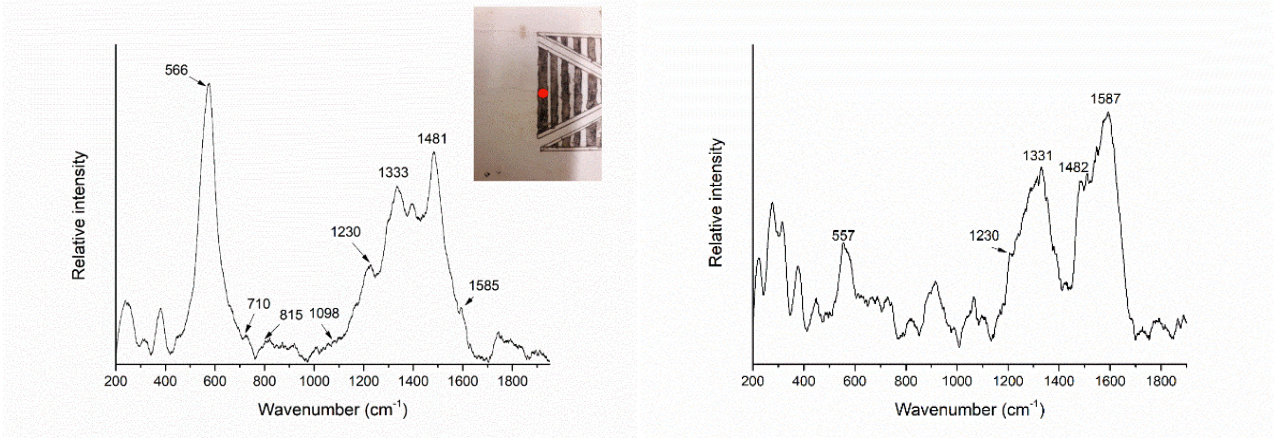

Figure 11 Representative RAMAN spectra of iron-gall ink. The enclosed image shows the point (red) of the front cover where the spectrum was collected (1R-ink-01). The right spectrum indicates a variable ink quantity but of same iron gall content

[4] Alum is sometimes known as potassium alum or potash alum in its pure form. Potash alum has the chemical formula $KAl(SO_4)_2 \cdot 12H_2O$ and the chemical name potassium aluminium sulphate. Potash alum or potassium alum is the most prevalent type of alum.

[5] Gelatin is derived from animal collagen, which is a protein found in connective tissues such as skin, tendons, ligaments, and bones. The hides and bones of certain animals, usually cows and pigs, are boiled, dried, treated with a strong acid or base, and lastly filtered to remove the collagen.

4.3 NIR results

4.3.1 A brief account on paper ingredients and past work

Paper is an industrial material, widely used in many everyday applications, and its study allows us to evaluate the raw materials used to produce it and evaluate the different processes its degradation. The main components are bonded fibers of cellulose that are linear polymers of glucose (β-D-glucopyranose) monomers linked by β-1,4-glycosidic bonds (Librando et al., 2011). (Fig.12)

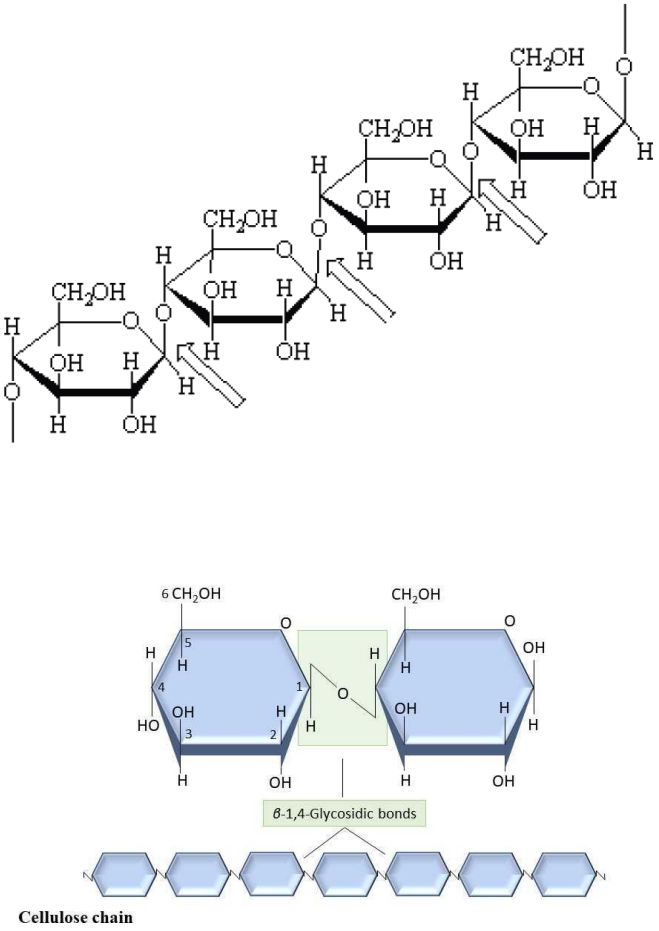

Figure 12. The β-1,4-glycosidic bonds of cellulose chain (after Libando et al., 2011)

The main chemical reactions that control the chemical properties of cellulose occur at hemiacetal bonding (glycosidic linkage) and/or hydroxyl groups, also affecting its crystallinity. Crystalline structure is promoted due to intramolecular hydrogen bonds that connect cellulose chains, forming aggregates, that may order up to 80% (crystalline form) of the total chains. The less oriented structure, comprise the 'amorphous' form of cellulose (Fengel & Wegener, 1989). The presence of water molecules highly affects the form of cellulose, due to its hydrophilic nature. Other constituents that participate in its composition are small amounts of organic material and inorganic additives.

Natural aging processes including the presence of moisture, light, oxidative agents or microorganisms, affect the chemical properties of the paper, triggering cellulose degradation, resulting in the reduction of the cellulose crystallinity (Browing, 1977).

In general, the study of ancient papers from the view of near infrared spectroscopy, regarding the paper composition and its degradation, the kind of the raw material that was used, as well as the composition of the pigmentations/inks, is quite limited. Their study using spectroscopic methods mainly focuses on Raman and FT-IR spectroscopy (Libando et al., 2011; Kostadinovska et al., 2013). Kostadinovska et al., (2013) examined the type of pigments (blue, red and white dye as well as black ink) in old Slavic specimens using Raman and FT-IR spectroscopy. Their results were overall based on Raman spectroscopy, as the FT-IR method applied to red dye and black ink had similar spectral characteristics. FT-IR spectroscopy, how-

ever, may indicate differences in the spectral properties of the materials used as raw, either in paper or in pulp. Very interesting approaches to answering these questions are the combined use of spectroscopy and statistics, and the study of spectral data through statistical analysis, as conducted by Jang et al. (2020), Lichtblau et al., (2008), Reháková et al., (2017), Trafela et al., (2007), Xin et al, (2014).

4.3.2 Discussing the NIR results

The spectral characteristics imprinted from the measurements of the ancient paper, by means of the SM-3500 Spectral Evolution portable spectrometer are summarized in the table below. From every page, at least 3 measurements were taken from different areas of the page (empty area, area with ink and paper, and area of the paper characterized by humidity).

At a first glance the collected spectra are in general similar, without any susceptible changes independently of the spot area. Even the presence of ink, in relation to the surface covered by the detector for receiving the spectrum, is too small, so that no distinct characteristics are observed that could be attributed to the presence of ink. Absorption characteristics representing the presence of cellulose were identified in all spectra, in the form of distinct absorptions (Fig. 13A). Further processing of the spectra by removing the background helps to discern some further details (Fig. 13B). In the spectra obtained from the regions of the paper that stand out for the presence of moisture, the formation of a more distinct feature is observed at 1370 nm (C-H stretching vibrations and C-H deformation vibrations), to the left of the deep intense absorption at 1490 nm. They are also characterized by a relatively smoother and bigger slope of their spectral signature in the range of 450 to 1100 nm (Table 2).

Table 2. Summary of the absorption characteristics with the main functional groups

Wavelength region	**Active molecular group**
1430 nm (cellulose)	First overtone of O-H stretching
1490 nm (cellulose)	First overtone of O-H stretching
1590 nm (cellulose)	First overtone of O-H stretching
1790 nm (cellulose)	First overtone of C-H stretching
1835 nm (cellulose)	O-H stretching and second overtone of C-O stretching
2100 nm (cellulose)	O-H stretching and C-H deformation
2270 nm (cellulose)	C-H stretching and C-H deformation
2336 nm (cellulose)	C-H stretching and C-H deformation
1370 nm (hemicellulose)	C-H stretching and C-H deformation
1700 nm (hemicellulose)	First overtone of C-H stretching
1940 nm (water)	O-H stretching and second overtone of C-H stretching

In the blank paper focusing spectra, there is a slight increase in the absorption depth at 1940 nm (O-H stretching vibrations relative to the presence of water and second overtone of C-H stretching vibrations) and at 2100 nm (O-H stretching vibrations and C-H deformation vibrations). In addition, the small features in the 1700 and 1790 nm regions (first overtone of C-H stretching vibrations) of the electromagnetic spectrum are generally more visible, in contrast to the spectra obtained from the other areas.

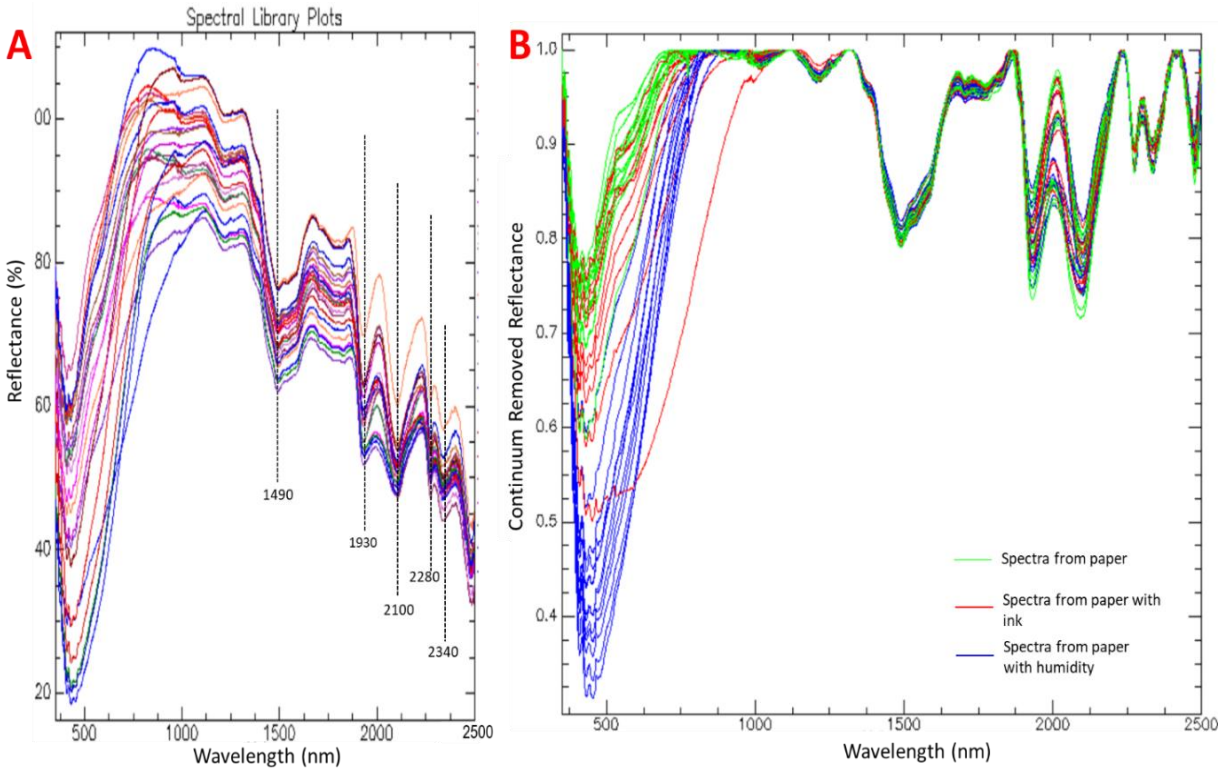

Figure 13. Representative spectra with the characteristic absorption features (A), and with continuum removed (B).

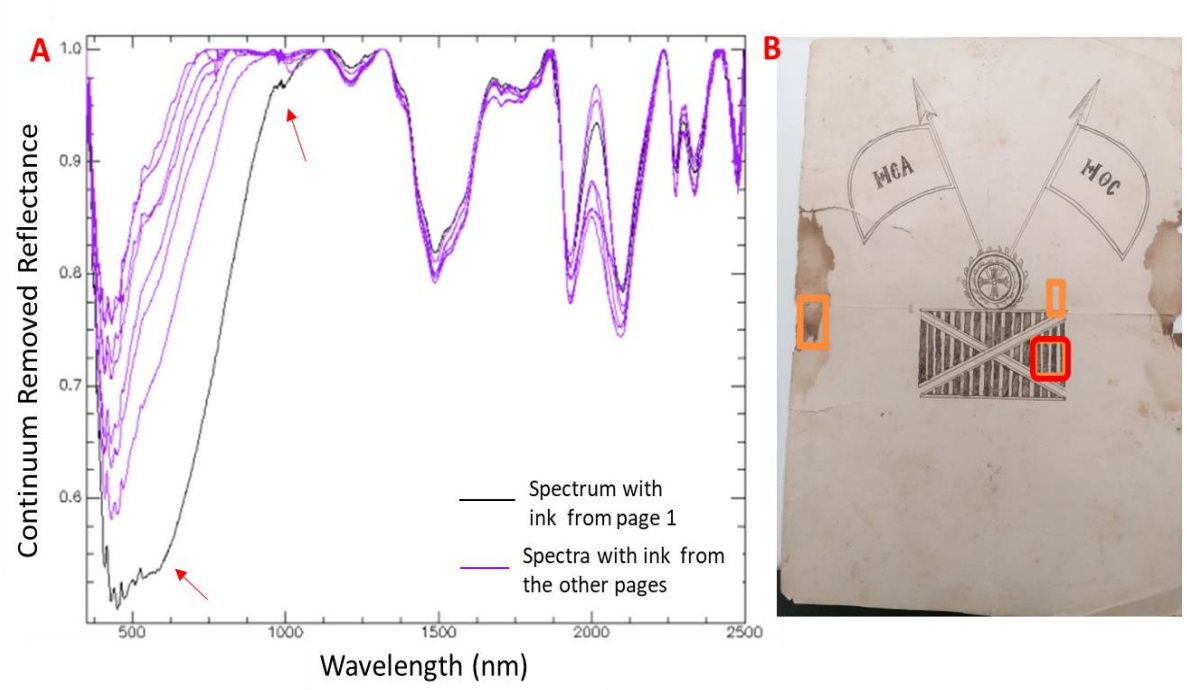

Figure 14. (A) Spectral features of paper with ink from page 1, in comparison with the other obtained spectra from areas with ink and (B) the areas of page 1 that were measured (paper with ink is the red box)

In detail observation of the spectra features acquired from areas rich in ink from the available pages, are clearly distinguished from the spectrum of a related area of the page 1 (Fig.14), where the continuum of the spectrum displays deeper absorption characteristics in the visible range of the electromagnetic spectrum, a steeper slope towards 1150 nm, and the small absorption features in this area are differentiated (indicated with arlines). This may be due to the fact that ink in page 1 is of variable quantity.

Furthermore, even though the absorption features and the spectral characteristics seem to be similar, with a closer look at the spectrum of page 3, a wavier continuum is observed from 350 to 1000 nm, and a small absorption feature at 550 nm approximately is developed. Similar characteristics, but to a lesser extent are observed at the spectra of page 2 (Fig. 15).

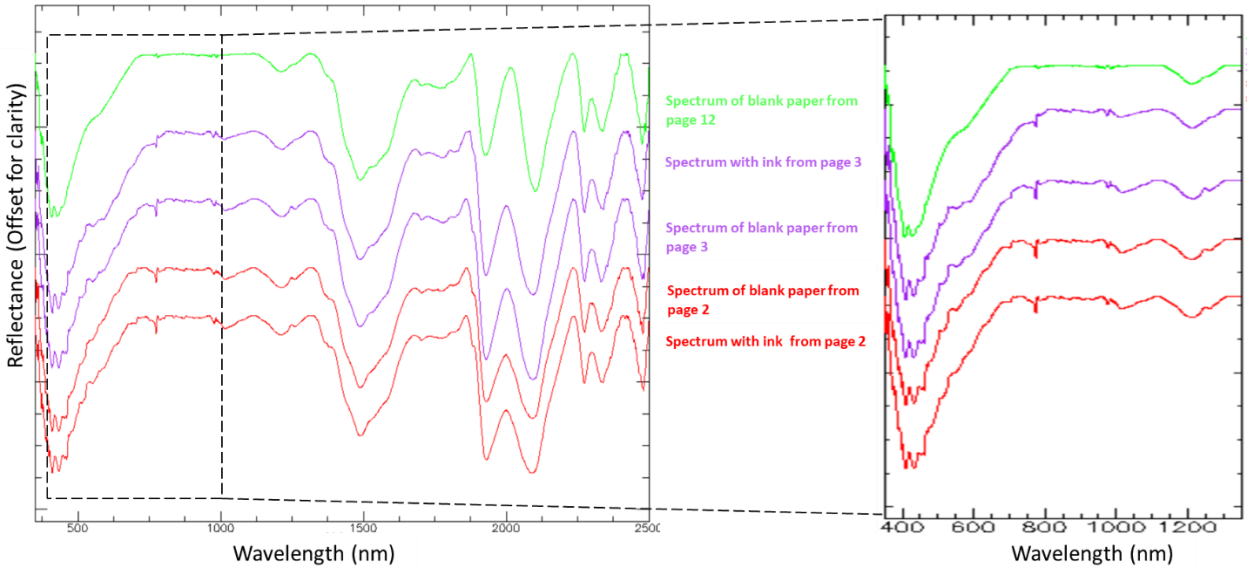

Figure 15. Reflectance spectra from blank paper and paper with ink of pages 2 and 3, compared with one randomly selected spectrum of blank paper (page 12).

The following diagrams give the variation of the characteristic absorptions observed at specific wavelengths of each measurement, in the regions of ca. 1930 and 2340 nm. As expected, different regions of the wavelength are affected variously (Fig.16).

The presence of moisture significantly affects the absorption positions at about 1930 nm, where the fluctuation is relatively more intense, while in this wavelength range the smallest variation occurs in the spectra that represent areas of paper with ink. (Fig.16A)

The presence of moisture also gives a shift of the wavelength to longer wavelengths, the absorption at about 2340 nm, while in the other two cases of ink and paper alone, the variation moves to shorter wavelengths (Fig.16B). At any rate within the errors these absorptions for the three cases center to ~1930 and ~2340 nm.

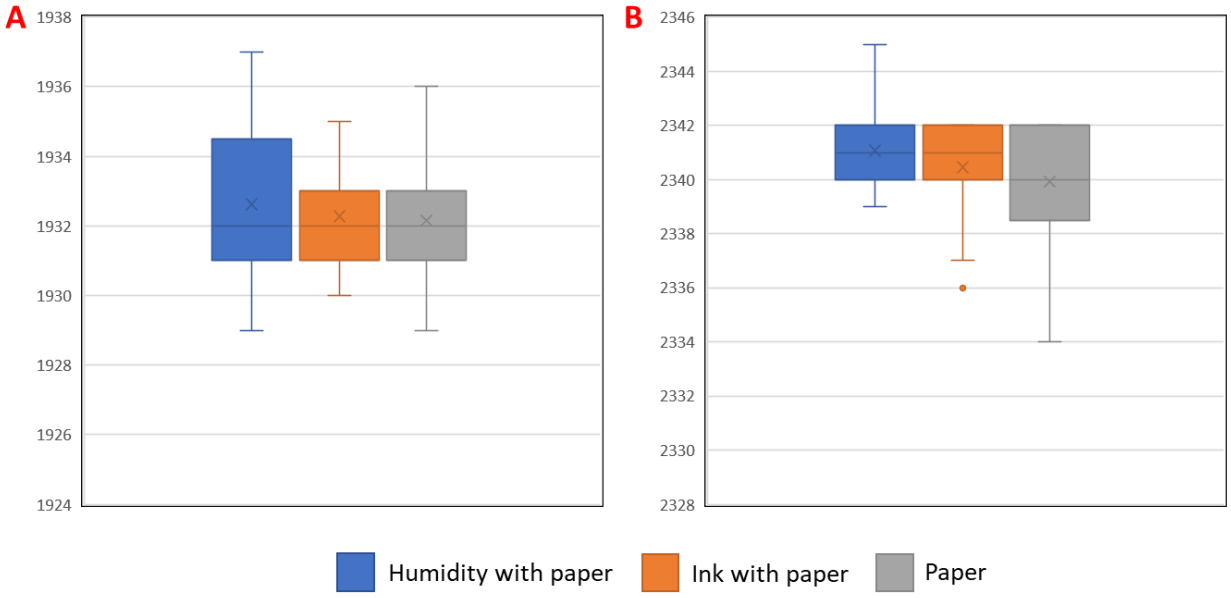

Figure 16. Boxplot diagrams representing the deviation of the wavelength values of the absorption features at ~1930 (A) and 2340 nm (B).

In addition, in order to understand the spectral signatures, samples were collected from modern industrial white paper ('global office paper'), as well as from an old essay paper dating to around 1850, aiming at the comparison of the results, as shown in Figure 17, where they are compared with 2 representative spectra from the ancient essay. The spectral signature of modern white paper resembles the absorption characteristics of the spectral signatures obtained from the ancient essay.

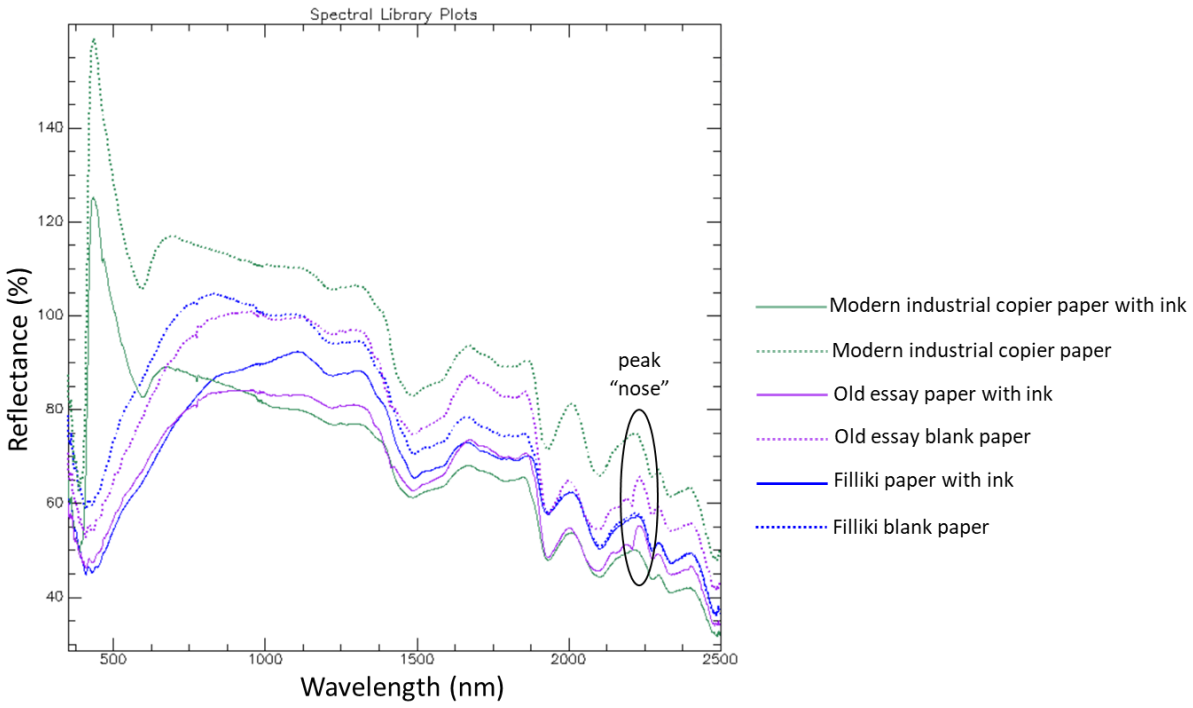

Figure 17. Representative diagrams of different paper samples

Their difference is mainly recognized in the visible range of the wavelength; in lieu, in the slope of the spectrum of the modern paper, intense and sharp absorptions are recorded, which were not observed in any other spectral measurement in the ranges between 385 and 595 nm.

On the other hand, the spectral signatures collected from the papers of the old book are similar, however they are characterized by a differentiation in the region at 2200 nm, where two small absorption characteristics are observed at these wavelengths, at approximately 2160 and 2210 nm, followed by the abrupt elevation of the spectral characteristics forming a kind of 'nose'. An additional absorption characteristic detected in these spectra, of fairly low intensity, is detected at about 1415 nm.

The explanation is that with NIR the material used as a raw material for the construction of the papers seems to be common, as no characteristic differences in the absorptions observed in the spectral signatures of the sample under study were observed. Only slight differences for the three first pages are observed. The fact NIR covers a large spot with blank paper and ink this produces issues and only small variations are perceptible.

4.4 Radiocarbon (C-14) dating results

The two C14 data and plots from the Calib 8.2 calibration using the IntCal20 dataset (Reimer et al., 2020) are given in Tables 1, 2 and Fig 19. The second run was simply to see if the extra step would make any difference, and in fact it did not: the bleach date is 10 years older, but that shift is less than one standard deviation.

Two processed sub-samples of Fig.18 gave the results of Tables 3 and 4 and respective plot in Fig.19a, b.

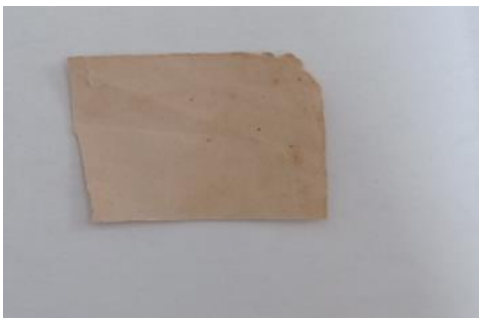

Figure 18. The paper sample analyzed (~2x1.3 cm).

Table 3. Sub-sample 1 radiocarbon analysis

Radiocarbon Age BP 145 ± 15		
Calibration data set: intcal20.14c, Reimer et al. 2020		
% area enclosed	cal AD age ranges	relative area under probability distribution
68.3 (1 sigma)	1682- 1695	0.149
	1724- 1738	0.154
	1754- 1761	0.068
	1800- 1811	0.127
	1837- 1845	0.071
	1851- 1867	0.111
	1871- 1878	0.066
	1916- 1939	0.253
95.4 (2 sigma)	1672- 1700	0.153
	1721- 1766	0.224
	1772- 1778	0.014
	1798- 1815	0.108
	1833- 1890	0.284
	1907- 1943	0.219

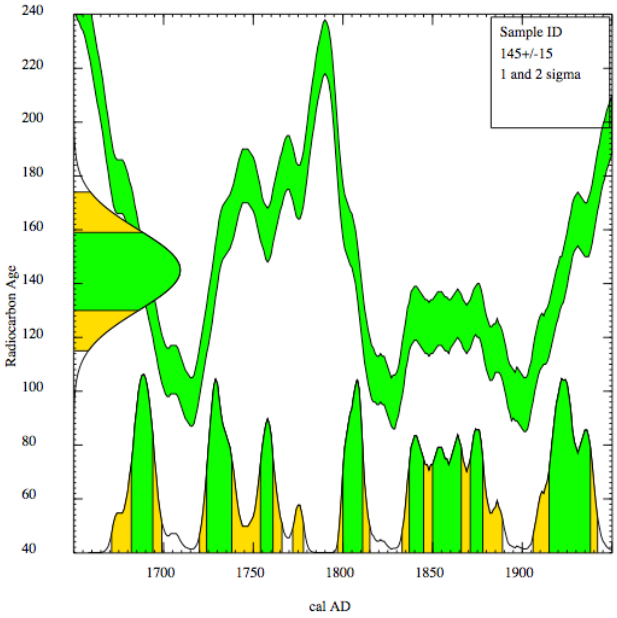

Figure 19A. Radiocarbon ages (vertical axis) versus corrected (Cal) ages (horizontal axis). The bell curve on the vertical axis gives the time before today (145 years ±15 years BP). The age 145 years is the peak of the curve. The green area and yellow area indicate the probability that the correct age is given with a degree of confidence of 68% and 95%. The uncorrected age as projected parallel to the horizontal axis intersects the internationally accepted calibration curve (green zig-zag) at several points which projected on the horizontal axis with the corrected ages gives the alternating curves on the horizontal axis - green and yellow i.e. confidence level of the corresponding intervals 68% and 95% respectively.

Table 4. Sub-sample 2 radiocarbon analysis.

Radiocarbon Age BP 135 ± 15		
Calibration data set: intcal20.14c, Reimer et al. 2020		
% area enclosed	cal AD age ranges	relative area under probability distribution
68.3 (1 sigma), cal AD	1686- 1698	0.131
	1722- 1731	0.086
	1806- 1813	0.081
	1835- 1881	0.514
	1885- 1887	0.007
	1909- 1926	0.180
95.4 (2 sigma), cal AD	1680- 1712	0.147
	1718- 1740	0.107
	1752- 1763	0.027
	1799- 1825	0.106
	1831- 1894	0.427
	1904- 1940	0.180

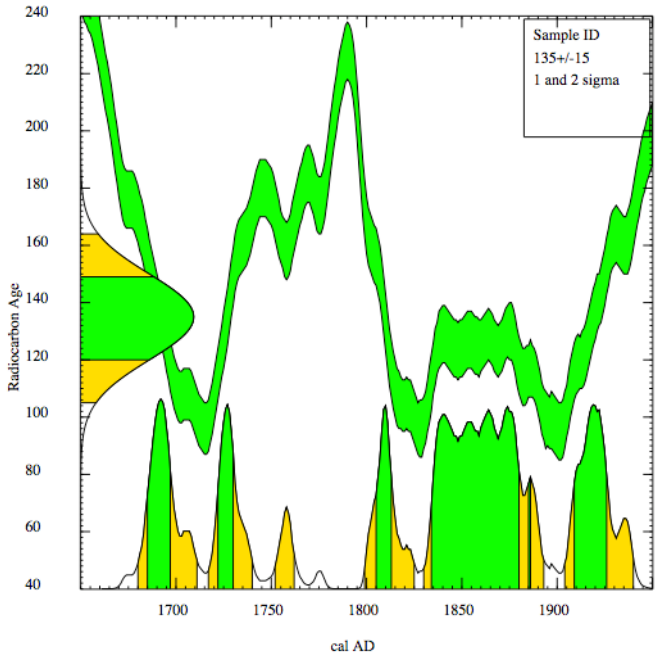

Figure 19B. Like Fig. 19A for the second shot the age of 135±15 years ago (1953 today).

For a 2sigma (95%) probability and dividing the probable period of writing into less than 1814 and later than 1814 (the date that Filiki Eteria was established in Odessa) the following probabilities for paper production are calculated from Table 5a,b.

Table 5. 2sigma(95%) probabilities and probable periods

Possible paper production age	probability	Age range	2sigma
TABLE 5A			
<1814	0.500	1672-1815	+
>1814	0.503	1833-1943	+
TABLE 5B			
<1814	0.387	1680-1825	+
>1814	0.607	1831-1940	+

The calendar date of paper production is unfortunately divided into almost two equally possible age ranges. Therefore, the C-14 result for the period concerned cannot assign with certainty the paper production which is of course earlier by an unknown time that the time or writing. Historical assessment below reinforces the date a few years after the organization was set up.

Radiocarbon unfortunately for the period after about 1600 to present day gives ages with a probability of more than three possible ages. The ups and downs of the calibration curve do not allow a definite result.

The results show that it was almost certainly not made from vegetation that grew in or just before 1800 AD: such material would produce 14C dates of around 200 BP, whereas our dates are 60 years younger.

The plots show that there's very little probability that the paper was made from biomass that grew in the period 1780-1800. However, if the text was written on archived or recycled paper from several decades earlier, or, the supposed historical date is a few years off and the writing was done in the very early 1800's on paper produced in (say) 1801 or 1802, the document is original. To the contrary the manuscript could be a later rewriting.

The paper in around 1800s has started been produced by pulpwood usually made by cellulose fibers from wood chips (like spruce, pine, fir, larch and hemlock, and hardwoods such as eucalyptus, aspen and birch) and less from recycled rag (cotton), straw, manila. The examined manuscript paper has been ascertained by visual examination of the paper against daylight where no striped lines neither watermark are observed, and moreover this paper absorbs ink as lettering is seen through the other side of the paper as mirrored shadow, having also the smooth surface shown from pulpwood.

Since the paper has been produced directly from the tree (wood pulp) material itself therefore the paper was produced from plant material that was photosynthesized at most a few years earlier. It follows that the ^{14}C date should correspond to a calendar date of the year of organic matter was cut, the paper production was made some time later (from one to few years) and the writing a few years later than the actual time of cutting the wood. At any rate, wood or rags would not likely be more than a few years old (a decade at the most).

In the early 1800s paper in Europe was made from linen or cotton fiber, mostly from recycled rags and first-time wood pulp has appeared. Full usage of wood in paper has been made only since the mid-1800s. Things started to get exciting in the world of paper between 1800 and 1850. First was the "mechanical pulping process" where forestry products are manufactured into paper pulp. This meant that rather than harvesting flax, trees were able to be used for making paper. Papers of the early 19th century were generally tan, or smoke colored, due to processing the rags using water with high iron content.

4.5 Fractal algorithms of individual words

Three analytical ways were applied. A) Full written page images of the handwritten manuscript pages b) For 5 lines images as being robust and avoids unwritten parts in a page, c) single words as RGB, repeated in different pages, d) single words as Gray-scale Minkowski Dimension analysis (an analytical account is given in Andronache et al., 2023).

In particular:

1. For full lines images images were converted from RGB to 8-bits gray-scale tiff uncompresed images, then, proper operators were applied. By using the Minkowski method, we analyzed the relationship between the words and the area occupied by it. The Minkowski dimension (D_M) is based on the Minkowski cover, which was first examined by Bouligand (1929) using morphological dilation. Then, the fractal size is calculated by analyzing the log-log curve of the area versus *r*.

D_M is determined using the formula

$$D_{M\,(r)} = 2 - \frac{\log A(r)}{\log r}$$

Where *A(r)* is the area of influence of the object with radius *r*.

In our research *r* has been set to 10 pixels. In fact, the higher the value, the closer the shape is to a perfect geometric shape. The lower the value, the more irregular the shape.

2. For 5 lines images, 5 complete lines were extracted from each analyzed full lines image, then fractal analyzes were performed with Minkowski Dimension algorithm.

3. For Words Firstly images were converted from RGB to 8-bits gray-scale tiff uncompresed images following application by certain operators

4. Gray-scale Minkowski Dimension analysis for words

The spatial relationship between the words and the paper on which they were written was analyzed by a) images were converted from RGB to 8-bits gray-scale tiff uncompresed images and b) then fractal analyzes were performed with Minkowski Dimension algorithm for binary images.

While in shape analysis, the Minkowski Dimension (D_M) approach considers two-dimensional space, for texture space is three-dimensional, due to the third coordinate corresponding to the intensity of the gray level at each point (Marana et al., 1999)

Using the Minkowski Dimension, the relationship between the object and the space it occupies is analyzed. The fractal size is obtained by calculating the volume of the dilated object.

Dilation can be accomplished by considering a sphere of radius r that is centered at each point of the original object and all other points within the sphere are joined to the object. To generate a "signature" for the shape, the volume of the object is analyzed as a function of r, using the exact distance transformation (EDT), which is the distance between all points in the image to the nearest point in the object. After that, the fractal size is calculated by analyzing the log-log curve of the influence volume with respect to r.

D_M is determined using the formula

$$D_{M\,(r)} = 2 - \frac{\log V(r)}{\log r}$$

Where *V(r)* is the volume of influence of the object with radius *r*.

In our research *r* has been set to 10 pixels; the higher the non-uniformity of the objects to be analyzed, the higher the Minkowski fractal size and vice versa. Software used were IQM 3.5 (Kainz et al., 2015).

4.6 Methodology for RGB analysis

For ink

1. Automatic image segmentation using WhiteBalance in IQM software. The background of the image (paper) turns white and the writing fades slightly.

2. Image binarization with ImageJ: white pixels represent the writing and black pixels represent the background (mask image).

3. Extraction of the writing to the real chroma, and the backgropund remains black, through the subtraction mathematical operator (it is extracted with the help of the mask image, from the original image). The new RGB image is created only with the color pixels of the ink.

4. create the RGB histogram of the image (only with the color pixels of the ink) in ImageJ.

5. Select which ink chrome is dominant and at the same time which has a central position in the letters and is darker.

6. Extract the pixels that have those three conditions listed above and determine the RGB value in IQM.

for paper

1.identify a part 40x40 pixels of the page unaltered by spots or shadows of the letters on the back,

2. the RGB value is determined in IQM.

Some characteristic images processed after cleaning from noise are given in Fig.20, and an example of the 5 lines text cleaned per page is given in Fig.21.

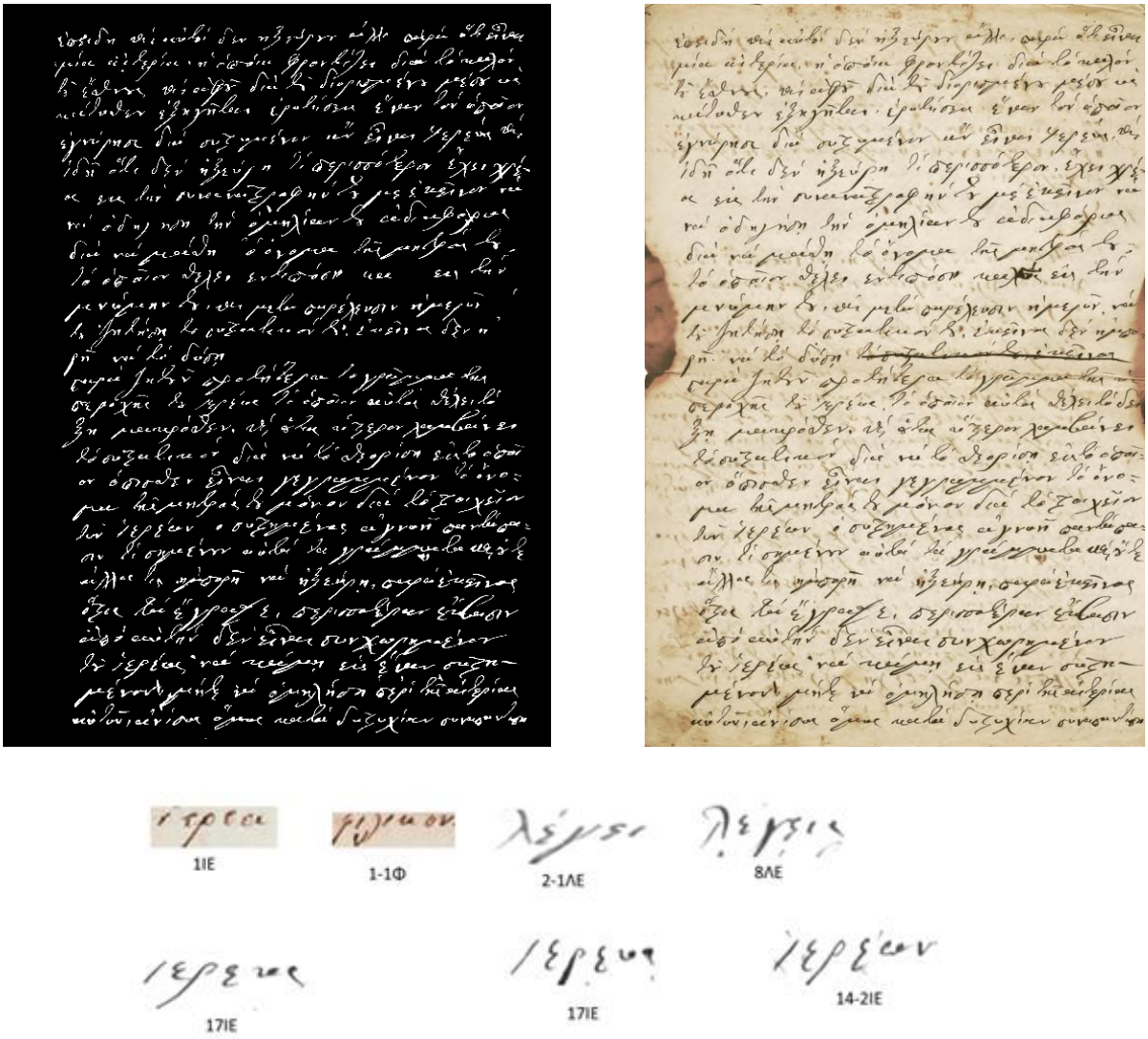

Figure 20: One written page (the 11th) and some words derived from specific page numbers (in front of their code) from the manuscript, cleaned from noise and processed by algorithms.

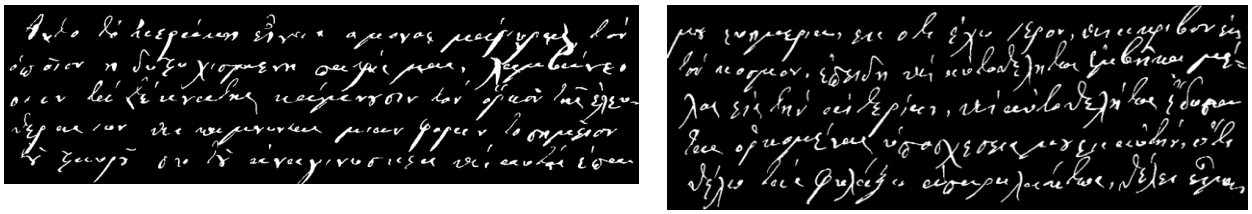

Figure 21: An example of the 5-lines text cleaned extracts from page 8 (left) and 19 (right)

4.7 Fractal processing results

The choice of words was taken randomly observing the most frequent occurrences throughout the manuscript. Articles (like definite the =την) are not conclusive due to low number of characters. These chosen words are recorded from the first written text of page 2 the confirmation letter. The Minkowski dimension D_M with dilation 10 data for single words and five lines and whole page per page is plotted (Fig.22).

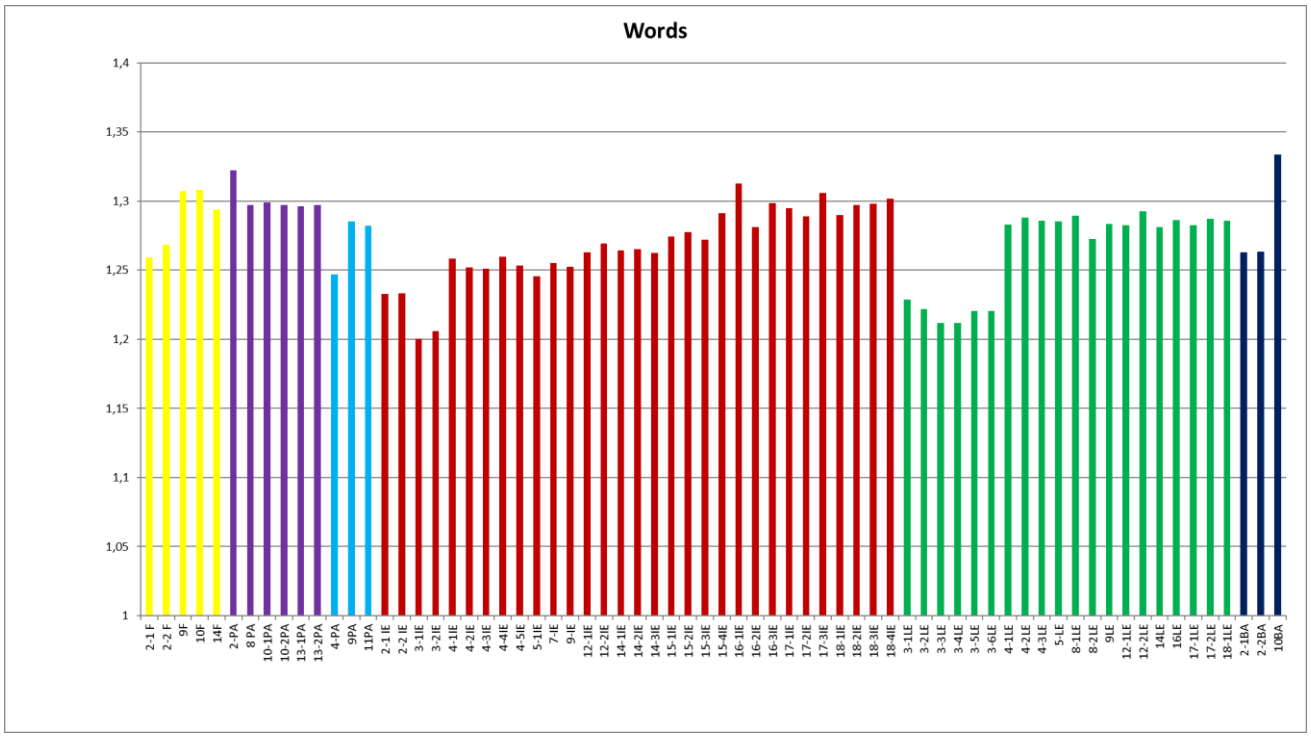

Figure 22. DM for each single word analysed. Code names are first the page number and in some cases more of these words in same page, followed by initial characters of the word. Yellow: φιλικός (friend), Mauve/Light Blue: Πατρίδα (homeland), Red: Ιερέας (priest), Green: λεγειν (saying), Dark Blue: βαθμός (rank)

For friendly/φιλικός (yellow) the page 2 differs from pages 8, 9, 13, which are grouped together. This implies a clear two authors.

For homeland/πατρίδα (blue), here we note that the different initial letter pi (π) even in same page in *patrida* is written alternatively as π or like omega  and this has some slight impact in the author's style interpretation. Thus pages 2, 8, 10, 13 are written with pi as omega (mauve) and 4, 9, 11 as pi (light blue). The 4 is part of an A3 size (4-7 pages) and the 8-11 and 12-15 are parts of A3 size paper. The page 2 (confirmation letter, D_M=1.33) is one author as is distinct from 8-13 pages (D_M=1.29) another 2nd author. Pages 9-11 (D_M=1.28) (with pi as omega) are close to 8-13 (with pi as omega). This implies another author writing 8-13 pages; for 8-13 is given (together with the rest of words) at a maximum possible possibility as written by same author together with 9-11 with a slight difference due to pi (π or ).

For priest/ιερέας (red) the pages 2 and 3 differ (D_M=~1.23 and 1.20 respectively). The pages 2 and 3 indicate a different author and from 4 to 15 (D_M=1.25-1.26) is another and from 16 and later pages (D_M=1.27-1.30) may be another author or the same who wrote 4-15 but on a haste mode. Thus at least 3 authors are identified.

For saying /λέγειν (green) the page 3 D_M=1.22 different from pages 4-17, D_M=1.25-1.29. Though 4-15 and 16-18 may appear as two different authors it is rather attributed to the free fast writing author. This implies two authors.

For rank/βαθμός (dark blue) page 2 D_M=1.26 differs from page 10 of D_M=1.33. This implies two authors. It could be same author writing with two different betas the initial letter of βαθμός.

Following the 5-lines analysis (Fig. 23), in the writing style on page 2 of the manuscript, the Minkowski dimension (D_M=1.23±0.011) was found to be more that 1SD different from pages 4-6 (D_M=1.31-1.32), and from page 3 which has D_M=1.29±0.017 and from pages 7-19, which have the highest fractal dimension (D_M>1.34). In fact, within 1SD the average D_M for 4-6 pages is 1.32±0.008 and for 8-19 is 1.36±0.01. This implies **four scribes** contributed to this manuscript.

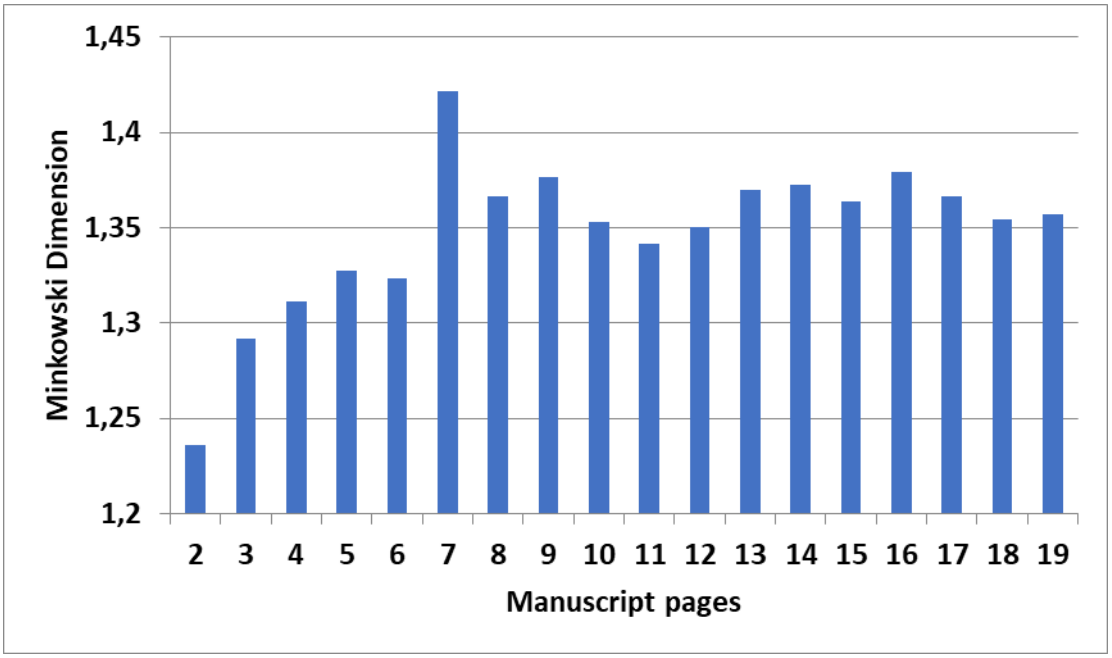

Figure 23. The 5-lines analysis per page 2 (confirmation letter) to 19 of the manuscript (Andronache et al., 2023).

Results for all pages, from page 2 to page 19, are displayed in Fig. 24. The trend is similar to the study of five lines per page (Fig. 23), but with a focus on whether the conditions we indicated elsewhere were satisfied (Andronache et al., 2023). Pages 2 (partially written and used to record the recommendation letter) and 7 (a page with a sparsely written cryptographic alphabet) provide a high and disproportionate rating scale. Pages 4, 5, and 6 all show one scribe and have an average D_M of 1.32 0.005. Page 7 has significant blank areas. Additionally, the pages 8 and later bear the notation D_M=1.350.01, indicating that another scribe, the binary mode representation of letters for similar words did have a tiny variance impact on the fractal analysis results due to the apparent quick writing style, but this does not rule out genuine variations. As a result, the same scribe is given credit for the writing. Accordingly**, at least two scribes** are suggested for all written pages due to the unfinished handwritten pages, which is undoubtedly not representative for the reasons stated above.

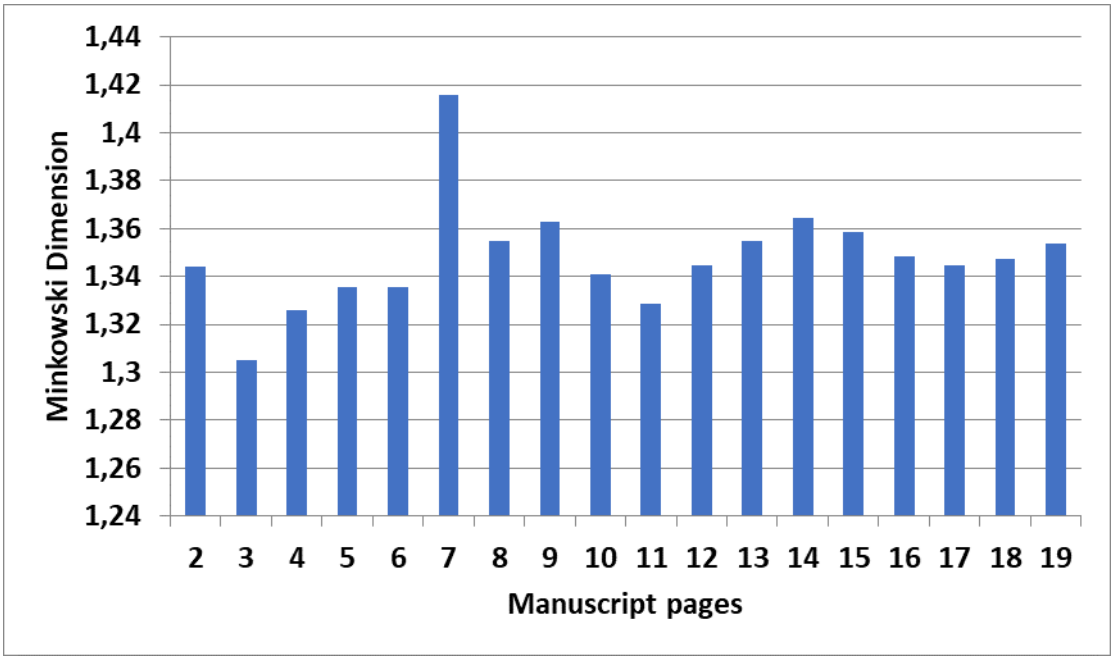

Figure 24. All lines in one page fractal analysis.

4.8 RGB of inks and paper

We examined inks color from 10 pages (1-14). We note that the ink color of the first cover page (front cover) is different from all. Inks from page 2 and from page 3 are again different between themselves and from all others. Inks from pages 4 and 5 to 14 are close or similar. We transform RGB in gray scale 8 Bits and obtain images with value between 0-255 grade where 0 is black and 255 is white. Our result in gray scale is the average of the R, G, B canals, and give a false impression of the intensity of the color but not the real color. If the average value is high means high luminance and low value is low luminance (darker). Thus, according to this RGB analysis four (4) different inks seem to have been used in the pages of the manuscript, for the pages 1, 2, 3, 4-14 (Fig.25); the 4-14 could be considered as one type of ink taken into account the variable errors attached due to the degradation of ink and paper.

In the pages we selected the dominant part without writing or visual degradation. From this part with its color histogram, we select a pixel in the dominant class as percentage (mean of histogram).

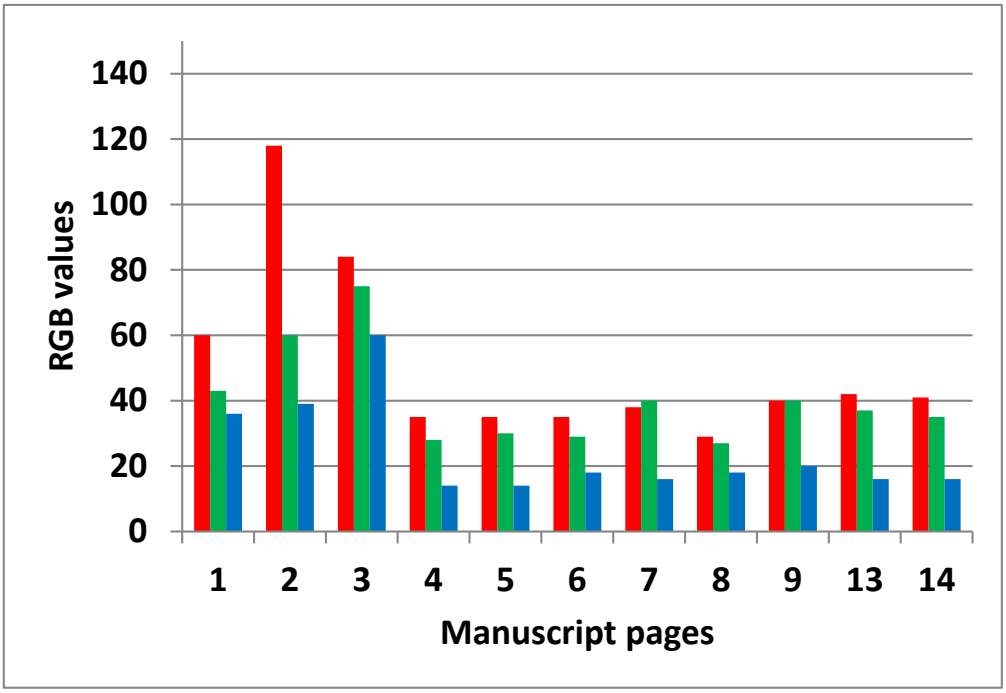

Figure 25. Histogram of 10 pages of the manuscript for their RGB values. Note 4 to 14 are similar ink, different from 1, 2, 3 and the 1-3 different themselves.

Regarding the paper material seems to be different in certain pages that is not coming from the same technique of paper production and ingredients. Because color of the pixels within a page varies and reflects alterations due to environmental factors and setting conditions all years through (e.g. exposure to humidity, light sources, oxidations from the inks etc.), it was chosen areas of 40x40 pixel in visually clear areas of a page whereas the area is as white as possible.

Fig. 26 gives the R, G, B for pages 1…to 20, where it appears paper have produced the result that indicates obvious differences in certain pages beyond the standard deviation. The different production technique and ingredients used applies at least for four (4) sets of pages 1st, 2nd, 3rd, 4th to 19th, 20th beyond standard deviation (see, Andronache et al., 2023).

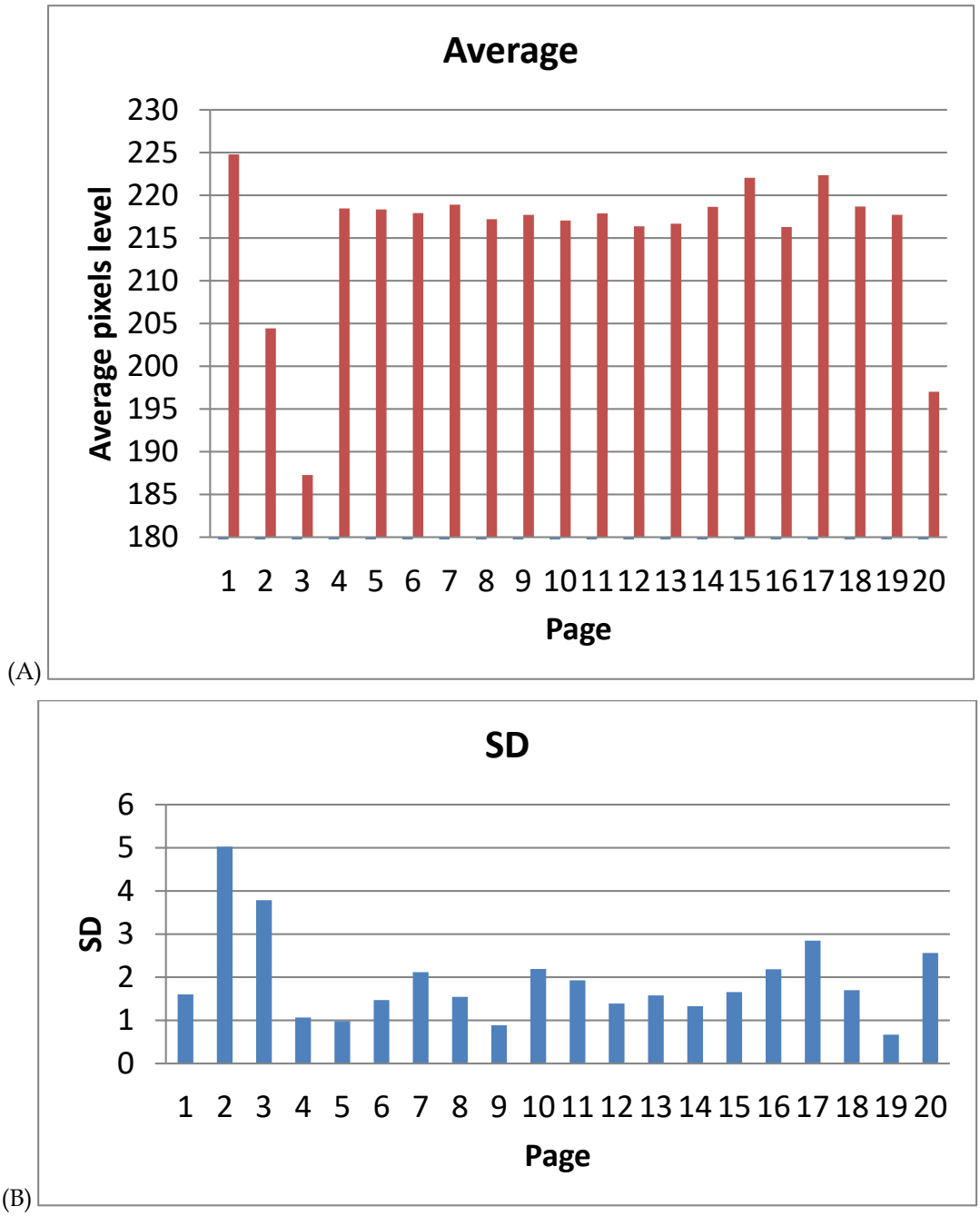

Figure 26. (A): Histogram of RGB for paper from pages 1 to 20. Image processing was made on 40x40 pixels areas per page. (B): standard deviation per page.

5. DISCUSSION & CONCLUSION

The complementary analytical techniques used to study the properties of this manuscript regarding number of possible authors, type of ink and paper, as well as dating produced extremely interesting results.

The XRF analysis and subsequent Dendrogram produced using Agglomerative Hierarchical Clustering (average method) identifies **four groups of inks** and paper in the 20 pages manuscript. The first three pages are different and possibly all others after the 4th. The 1st and 20th appear similar by XRF but in contrast to RGB. For the XRF the obtained readings may include adjacent paper because the X-rays spot ROI is around 1cm^2, hence we consider these values as semiquantitative. For future work our methodology should be applied using micro-XRF and averages of many letters of same page.

For the fractal dimension elaboration Minkowski D_M was used for words and lines as well as images of letters by converting from RGB to 8-bits gray-scale tiff uncompressed images. Some close D_M in pages for some words may reflect the slight change in writing

style and the spelling and grammar of the same author even the same page which occurs sometimes (e.g. for initials in some words π, ω, in word homeland/πατριδα, in the word society/εταιρεια as ετερεια, αἰτερία, ετεριa. At any rate fractal dimension is useful to identify **at least three authors** judging from the style of writing some individual words and/or several lines (at least 5) of text per page.

Five separate black iron gall inks were also identified by RGB image analysis of the ink and paper used on each page of the Greek manuscript (four for the written text and one including first page cover design). **Four scribes** were also identified from the findings of the 5-lines analysis. The identification of **five different paper types** is intriguing, as is the partial striking correlation between the inks, scribes, and papers on the same pages (e.g. 1, 2, 3, after 4, 20).

Regarding the ink used, the black ink that was used in medieval Europe is called **iron-gall ink**. There are hundreds of recipes for making iron-gall ink, but they have a few things in common. These things are gallnuts, iron vitriol (a. k. a. copperas), and gum arabic. Many recipes also use rainwater and wine. Early in the Middle Ages, the black ink was made from the carbon that was produced by burning wood. The **carbon** was scraped off and mixes with a paste made of tree gum and water. As the medieval era progressed, scribes altered their recipe for black ink. Moreover, in medieval manuscripts, we see several shades of red, indicating that different processes and components went into making the inks. Most commonly, the red ink from the medieval era was made from cinnabar, a natural, yet toxic, chemical compound of mercury sulfide, or HgS. Vermilion was also used in pigment, as well as other organic (e.g. Madder plant), or inorganic compounds (Gettens et al., 1972)

it is known that Ink corrosion causes two types of damage: reduced readability due to paper discolouration under and adjacent to the ink lines and local brittleness of the paper, which can result in cracks or even loss of material with handling; effects which require urgent conservation before they are digitized (Kostadinovska and Jakovleska Spirovska 2015; Gimat et al., 2021).

There are two main mechanisms in the iron gall ink corrosion that cause the degradation of the paper. The first mechanism is acid degradation resulting from a low pH level in the paper and acids from the ink. The second mechanism is an oxidation processes that are catalyzed by metal ions in the paper and the ink. In both degradation processes, the relatively flexible support - paper - becomes brittle and friable as a result of ageing complicated accompanied by the effect of apparently destructive (Melo et al., 2022)

Papermaking using pulp made from hemp and linen fibers from tattered clothing, fishing nets and fabric bags spread to Europe in the 13th century, with an ever-increasing use of rags being central to the manufacture and affordability of rag paper, a factor in the development of printing (Hunter 1943).

Until the 18th century the methods of making paper remained the same, but the raw materials were not enough and so the research turned to other directions for the discovery of new materials for making paper, but also for its mechanical making because until then paper was made. by hand and this slow method was financially unprofitable. By the 1800s, production demands on the newly industrialized papermaking and printing industries led to a shift in raw materials, most notably the use of pulpwood and other tree products which today make up more than 95% of global pulp production. For the production of paper, they crushed the raw material in water (linen, cotton, straw, wood) and for the grinding they used a manual grinder with wooden mallets. Towards the end of the 13th century, in Fabriano, Italy, they used the power of water to move metal pistons to mash wet material.

The use of wood pulp and the invention of automatic paper machines in the late 18th- and early 19th-century contributed to paper's status as an inexpensive commodity in modern times. (Hunter, 1943; Burger 2007, Ragnar et al 2014). While some of the earliest examples of paper made from wood pulp include works published by priest Jacob Christian Schäffer in 1765 who recommended the use of wood for making pulp and Matthias Koops in 1800 (Koops 1801, Hunter, 1943, Leong 2020, Sjöström,1993). Many new methods of making pulp were subsequently developed, which replaced the old methods. The present manuscript belongs to this pulpwood type of paper. Large-scale wood paper production began in the 1840s with unique, simultaneous developments in mechanical pulping made by Friedrich Gottlob Keller in Germany 1846 (Pönicke, 1997) and by Charles Fenerty in Nova Scotia. (Burger 2007).

Finally, the dating of the manuscript by radiocarbon gave probable age ranges due to the fact of wiggly character of calibration curve after 1600 AD.

The calendar date of paper production is unfortunately divided into almost two equally possible age ranges of higher and lower than 1814 (probability 0.5) with the establishment of Friendly Society in Odessa. Therefore, the ^{14}C result for the period concerned cannot assign with certainty the paper production which is of course earlier by an unknown time that the time or writing. However, historical assessment indicated by the written date of initiation the name and the place (island of Hydra) reinforces the date a few years after the organization was set up that is in 1819.

Author Contributions: Conceptualization, I.L.; methodology, I.L., I.A., I.I.,; software, I.A., I.I., M.K., V.X.; validation, I.A., I.I., M.K., V.X.; formal analysis, I.A., I.I., M.K., V.X; investigation, I.L., I.A., I.I., M.K; resources, I.A., I.I.; data curation, I.A., I.I., M.K., V.X.; writing—original draft preparation, I.L.; writing—review and editing, I.L., I.I., M.K; visualization, I.A., I.I; supervision, I.L.; project administration, I.L.; funding acquisition, none. All authors have read and agreed to the published version of the manuscript.

ACKNOWLEDGEMENTS

I.L. thanks the Grand Lodge of Greece for permission to study the manuscript and is thankful for support of the Sino-Hellenic Academic Project (www.huaxiahellas.com) from Key Research Institute of Yellow River Civilization and Sustainable Development & Collaborative Innovation Center on Yellow River Civilization of Henan Province, Henan University, Kaifeng, China. I.A. is thankful for support of the grant from the Romanian Ministry of Education and Research, CNCS - UEFISCDI, project number PN-III-P4-ID-PCE-2020-1076, within PNCDI III, grant of the Ministry of Research, Innovation and Digitization, CNCS/CCCDI-UEFISCDI, project number PN-III-P2-2.1-SOL-2021-0084. I.L thanks Dr G. Boudalis for discussion on paper production and inks, writing style, to Dr Ch. Karanasios for issues of writing style and techniques of inks and paper, and Dr A. Katopodis for communication on historical issues. We thank Prof. T. Levy for covering the cost of the C-14 dating.

REFERENCES

Andronache, A., Liritzis, I and Jelinek, H.F (2023) Fractal algorithms and RGB image processing in scribal and ink identification on an 1819 secret initiation manuscript to the "Philike Hetaereia". *Scientific Reports*, 13:1735, https://doi.org/10.1038/s41598-023-28005-4, 22p.

Browing B.L. (1977) *Analysis of Paper*, Marcell-Dekker, New York.

Barrett, T., Ormsby, M., and Lang, J.B. (2016) Non-Destructive Analysis of 14th–19th Century European Handmade Papers, *Restaur.*,37(2), pp. 93–135.

Bouligand, C (1929) Sur la notion d'ordre de mesure d'un ensemble plan, *Bull. Sci. Math.* 2, pp. 185–192.

Burger,P (2007) *Charles Fenerty and his Paper Invention*. Toronto, PB Publishing Inc, Canada. pp.25–30

Carter E A., Perez Fernando Rull, Garcia J. M. and Edwards H. G. M. (2016) Raman spectroscopic analysis of an important Visigothic historiated manuscript. *Phil. Trans. R. Soc. A*., 374, 20160041 20160041, http://doi.org/10.1098/rsta.2016.0041.

Fengel D., Wegener G. (1989). *Wood Chemistry, Ultrastructure, Reaction*, Walter de Gruyter, Berlin

Hortense de la Codre, Marie Radepont, Jean-Philippe Échard, Oulfa Belhadj, Stéphane Vaiedelich, et al., (2020) The use of XRF imaging for the chemical discrimination of iron-gall ink inscriptions: A case study in Stradivari's workshop. *X-Ray Spectrometry*, pp.1-9. 10.1002/xrs.3160. hal- 02569884.

Hunter, D (1943). *Papermaking, the history and technique of an ancient craft*. Dover, NY.

Jang et al., (2020). Korean traditional paper & NIR, *BioResources* 15(4), 9045-9058.

Gettens, R.J., Feller, R.L., Chase, W.T (1972) Vermilion and Cinnabar, *Studies in Conservation,* Vol. 17, No. 2, pp. 45-69.

Gimat, A., Michelin, A., Massiani, P. et al. (2021) Beneficial effect of gelatin on iron gall ink corrosion. *Heritage Sci.*, 9, 125, https://doi.org/10.1186/s40494-021-00593-2.

Kostadinovska, M., Jakovleska-Spirovska, Z., & Minčeva-Šukarova, B., (2013). A spectroscopic study of inks from a rare Old Slavic manuscript: Liturgical Collection of chronicles, scriptures, etc., *2nd Virtual International Conference on Advanced Research in Scientific Areas*, December 2-6, DOI: 10.13140/RG.2.2.11773.56808.

Kostadinovska, M and Jakovleska Spirovska, Z (2015) Implementation of methods for examination of paper-based library materials*, Vjesnik bibliotekara Hrvatske* 58, 3 / 4, pp. 119-133.

Kainz P., Mayrhofer-Reinhartshuber M, Ahammer H. (2015) IQM An Extensible and Portable Open Source Application for Image and Signal Analysis in Java. *PLoS ONE*, 10(1), e0116329, doi: 10.1371/journal.pone.0116329 (2015).

Katopodis A, (2021*) Aspects of the history of Greek Freemasonry*, Aggelakis Press, Athens (in Greek)

Koliopoulos J.S (1987). *Brigands with a Cause: Brigandage and Irredentism in Modern Greece, 1821–1912*. New York: Clarendon Press of Oxford University Press.

Koops, M (1801), *Historical account of the substances which have been used to describe events, and to convey ideas from the earliest date to the invention of paper*, London, Printed by Jacques and Co.

Librando, V., Minniti, Z., & Lorusso, S., (2011). Ancient and modern paper characterization by FTIR and Micro-Raman spectroscopy. *Conservation Science in Cultural Heritage*, 11(1), pp. 249–268. https://doi.org/10.6092/issn.1973-9494/2700.

Lichtblau, D., Strlič, M., Trafela, T., Kolar, J., & Ander M., (2008). Determination of mechanical properties of historical paper based on NIR spectroscopy and chemometrics – a new instrument. *Applied Physics*, DOI: 10.1007/s00339-008-4479-1.

Leong, E (2020). An Early Modern DIY Guide to Making Paper. *Hypotheses*, The Recipes Project. https://recipes.hypotheses.org/8447, Retrieved 2020-04-15.

Marana A.N, Da Fontoura Costa L., Lotufo R.A., Velastin S.A, Estimating crowd density with Minkowski fractal dimension (1999) *Proceedings of IEEE International Conference on Acoustics, Speech, and Signal Processing*, 3521-3524, DOI: 10.1109 / ICASSP.1999.757602.

Mazarakis-Aenian, I (2008) *The Filiki Etaeria*. Publ. Historical and Ethnological Society of Greece, Athens (in Greek).

Melo, M.J., Otero, V., Nabais, P. et al. (2022) Iron-gall inks: a review of their degradation mechanisms and conservation treatments. *Heritage Science* 10, 145, https://doi.org/10.1186/s40494-022-00779-2.

Pönicke, H (1977). "*Keller, Friedrich Gottlob*". *Neue Deutsche Biographie*. Berlin: Duncker & Humblot.

Phillips, W. Al. (1897) *The war of Greek independence, 1821 to 1833*, London: Smith, Elder.

Proost, K., Janssens, K., Wagner, B., Bulska, E and Schreiner, M (2004) Determination of localized Fe^{2+}/Fe^{3+} ratios in inks of historic documents by means of μ-XANES, *Nucl. Instrum. Methods Phys. Res.* B, 213, pp. 723-728.

Panagiotopoulos B.P (1964) The masons and the Filiki Eteria. Emm. Xanthos and Pan. Karagiannis, *The Gleaner,* Vol 2 (in Greek) doi: 10.12681/er.9648 e-Publisher: EKT, (Downloaded: 08/04/2022).

Pythagoras (2016) Historical token of the "Friendly Society" (ιστορικό τεκμήριο φιλικής εταιρείας), *Pythagoras Tectonic Bulletin of the Grand Lodge of Greece* vol.106, pp. 6-27.

Rath, J (1964), The Carbonari: Their Origins, Initiation Rites, and Aims, *The American Historical Review*, 69 (2), pp.353–370, doi:10.2307/1844987.

Reimer et al. (2020) The IntCal20 Northern Hemisphere radiocarbon age calibration curve. *Radiocarbon* 62, doi: 10.1017/RDC.2020.41.

Reháková, M., Gál, L., Belovičová, M., Oravec, M., Dvonka, V., Stojkovičová, D., & ˇCeppan, M., (2017). Identification of iron-gall inks in historical drawings by Fibre OpticsReflection Spectroscopy – Extension to the NIR spectral range. *Journal of Cultural Heritage*, Vol. 27, pp. 137-142. http://dx.doi.org/10.1016/j.culher.2017.03.005.

Ragnar, M., Henriksson, G., Lindström, M. E., Wimby, M., Blechschmidt, J., Heinemann, S (2014), "*Pulp*", *Ullmann's Encyclopedia of Industrial Chemistry*, Wiley-VCH Verlag GmbH & Co. KGaA, pp. 1–92, Doi:10.1002/14356007.a18_545.pub4, ISBN 978-3-527-30673-2

Schäffer, J.C (1765), Versuche und Muster ohne alle Lumpen oder doch mit einem geringen Zusatze derselben Papier zu machen (Regensburg, 1765), 33.

Sjöström, E. (1993). *Wood Chemistry: Fundamentals and Applications*. Academic Press.

Trafela, T., Strlic, M., Kolar, J., Lichtblau, A.D., Anders, M., Mencigar, P.D., & Pihlar, B., (2007). Nondestructive Analysis and Dating of Historical Paper Based on IR Spectroscopy and Chemometric Data Evaluation, *Analytical Chemistry* 79(16), pp. 6319-6323.,

Xin, Li-P., Chai, Xin-S., Barnes, D., Chen, Chun-X., & Chen, Run-Q., (2014) Rapid Identification of Tissue Paper Made from Blended Recycled Fibre by Fourier Transform near Infrared Spectroscopy, *J. Near Infrared Spectrosc.*, 22, pp. 347–355.